C&EN Supplement
SERVING THE CHEMICAL, LIFE SCIENCES & LABORATORY WORLDS

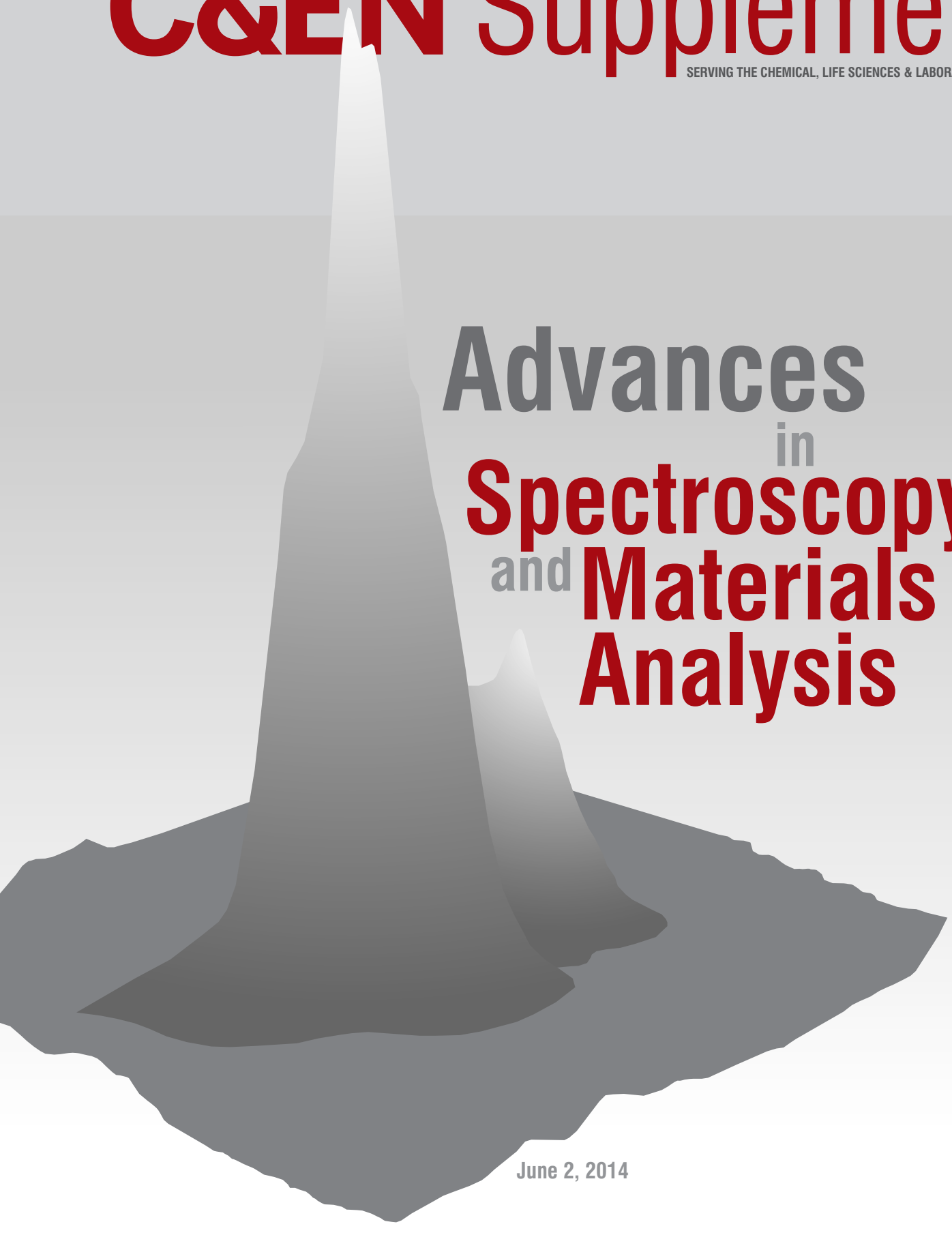

Advances in Spectroscopy and Materials Analysis

June 2, 2014

EMD MILLIPORE

Solutions for Mass Spectrometry

Leading the way for over a century

Chromatography solutions of the highest quality based on our customers' needs. This is what we have offered since 1904. This is why EMD Millipore's columns, plates and mobile phases are used in mass spectrometry labs throughout the world today.

To learn more about our leading solutions, such as our new HPLC columns, TLC/HPTLC MS-grade plates, and ICP-MS standards, please contact your EMD Millipore sales representative, or visit:

www.emdmillipore.com/mass-spectrometry

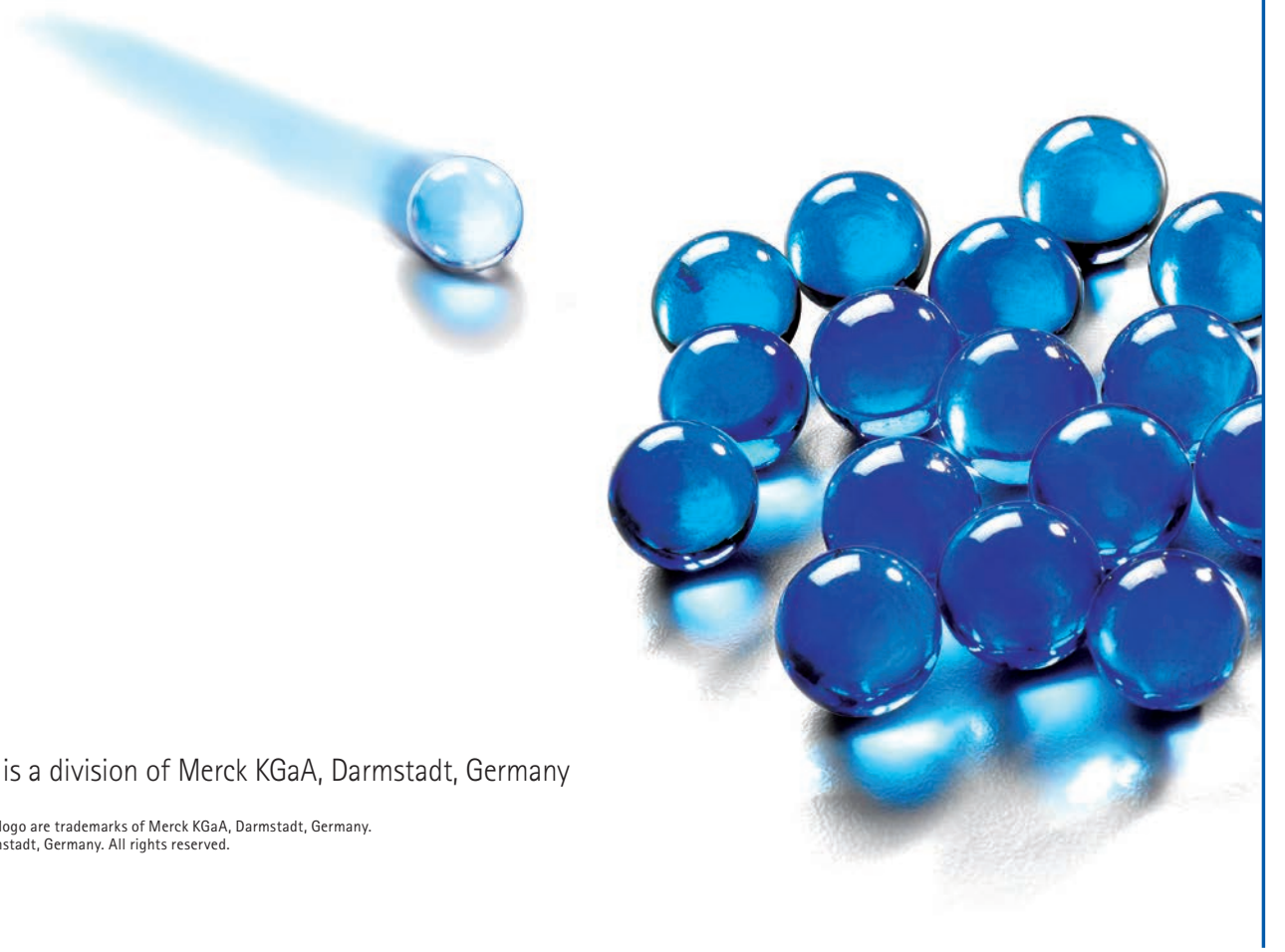

EMD Millipore is a division of Merck KGaA, Darmstadt, Germany

MERCK MILLIPORE

Solutions for Mass Spectrometry

Leading the way for over a century

Chromatography solutions of the highest quality based on our customers' needs. This is what we have offered since 1904. This is why Merck Millipore's columns, plates and mobile phases are used in mass spectrometry labs throughout the world today.

To learn more about our leading solutions, such as our new HPLC columns, TLC/HPTLC MS-grade plates, and ICP-MS standards, please contact your Merck Millipore sales representative, or visit:

www.merckmillipore.com/mass-spectrometry

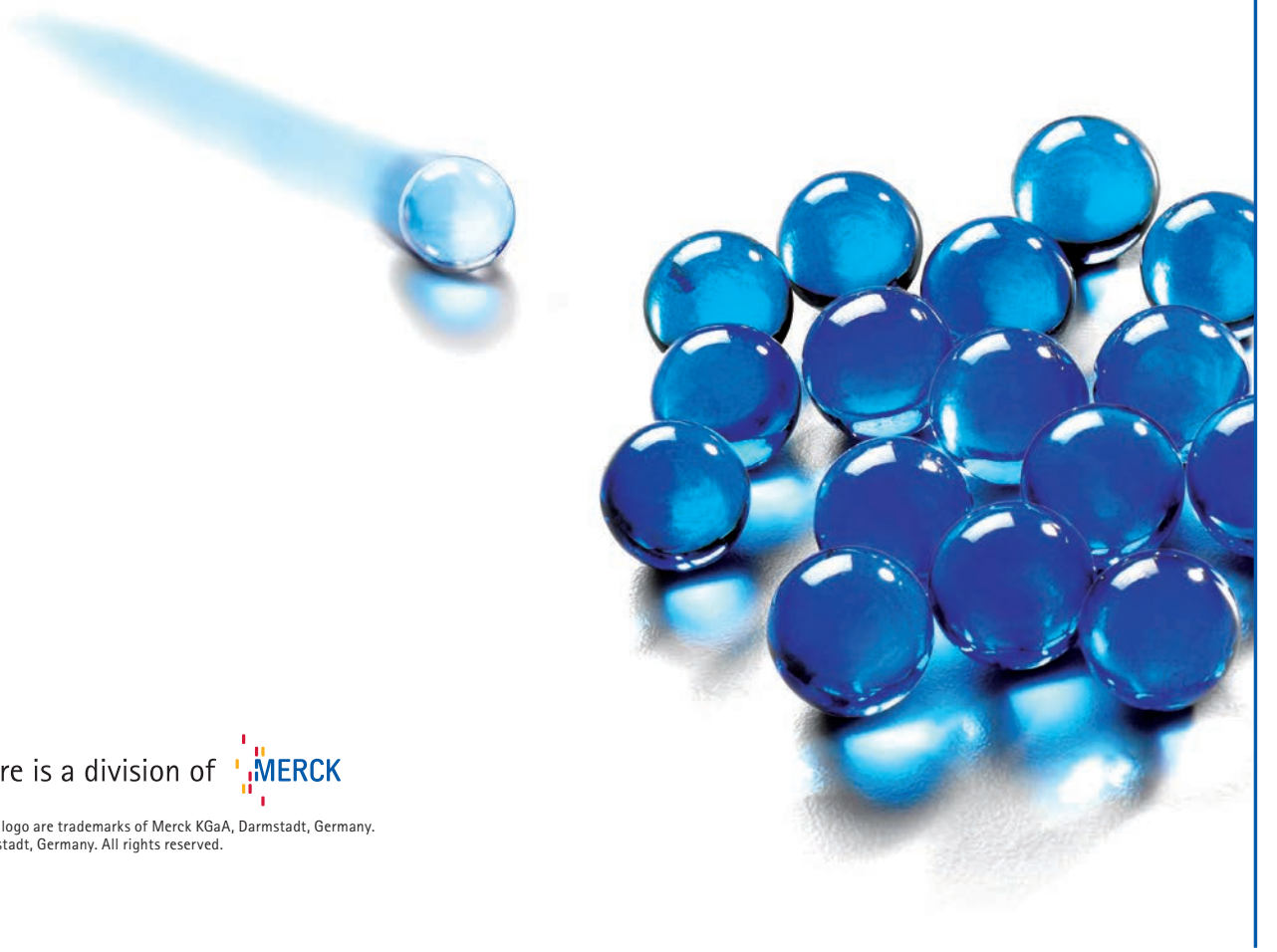

Merck Millipore is a division of MERCK

June 2, 2014

A SUPPLEMENT TO
C&EN
CHEMICAL & ENGINEERING NEWS

Advances in Spectroscopy & Materials Analysis

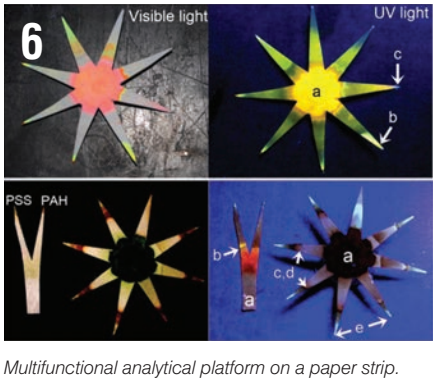

Multifunctional analytical platform on a paper strip.

First Issue Now Available Online »»

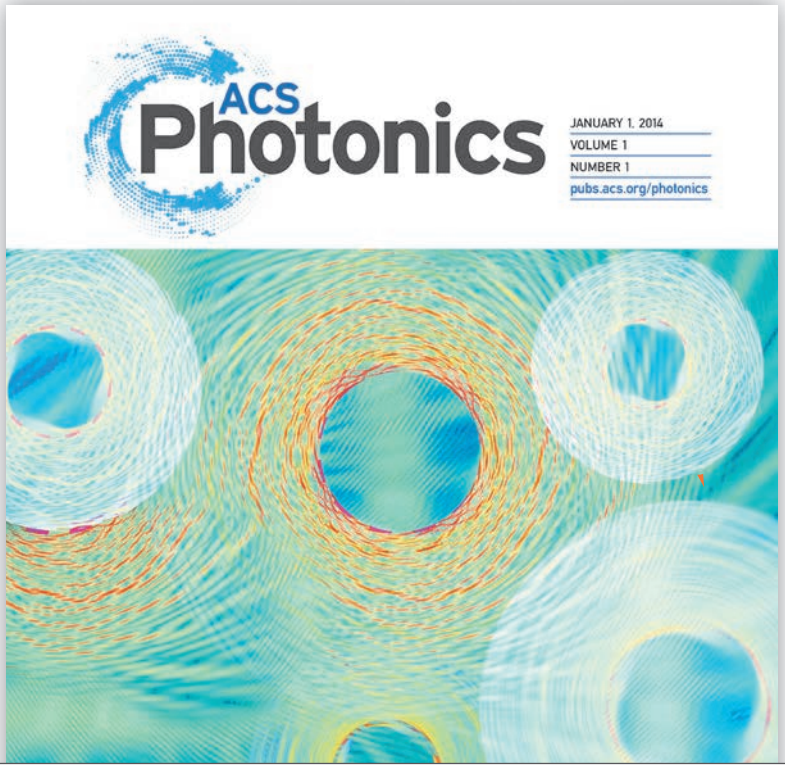

ACS Photonics is an interdisciplinary journal dedicated to publishing high-impact research that addresses emerging issues in the area of photonics. Read the first set of articles available online from the journal, freely accessible to all readers for a limited time.

Harry A. Atwater
Editor-in-Chief
California Institute of Technology

Teri W. Odom
Executive Editor
Northwestern University

For FREE access to the articles go to bit.ly/acsphotonics

Sign up for free e-Alerts to be notified when new articles post

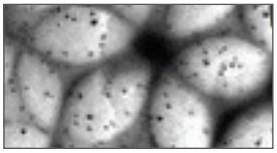

Three-Phase Co-assembly: In Situ Incorporation of Nanoparticles into Tunable, Highly Ordered, Porous Silica Films
Yolanda Vasquez, Mathias Kolle, Lidiya Mishchenko, Benjamin D. Hatton, and Joanna Aizenberg
DOI: 10.1021/ph400067z

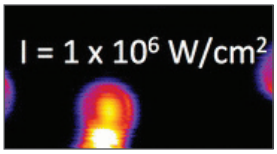

Saturation and Reverse Saturation of Scattering in a Single Plasmonic Nanoparticle
Shi-Wei Chu, Hsueh-Yu Wu, Yen-Ta Huang, Tung-Yu Su, Hsuan Lee, Yasuo Yonemaru, Masahito Yamanaka, Ryosuke Oketani, Satoshi Kawata, Satoru Shoji, and Katsumasa Fujita
DOI: 10.1021/ph4000218

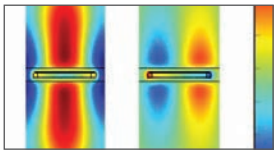

Tailoring Dispersion and Eigenfield Profiles of Plasmonic Surface Lattice Resonances
Aimi Abass, Said Rahimzadeh-Kalaleh Rodriguez, Jaime Gómez Rivas, and Bjorn Maes
DOI: 10.1021/ph400072z

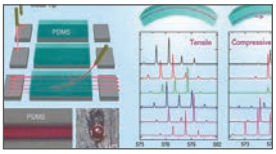

Bending-Induced Bidirectional Tuning of Whispering Gallery Mode Lasing from Flexible Polymer Fibers
Rui Chen, Van Duong Ta, and Handong Sun
DOI: 10.1021/ph400084s

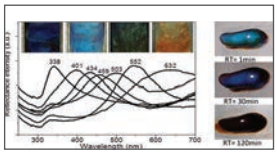

Tunable Lyotropic Photonic Liquid Crystal Based on Graphene Oxide
Peng Li, Minhao Wong, Xi Zhang, Haiqing Yao, Ryohei Ishige, Atsushi Takahara, Masahiro Miyamoto, Riichi Nishimura, and Hung-Jue Sue
DOI: 10.1021/ph400093c

ADVERTISER INDEX

A SUPPLEMENT TO
C&EN
CHEMICAL & ENGINEERING NEWS

This C&EN Supplements is produced by C&EN, the flagship magazine of the American Chemical Society.

American Chemical Society, 1155 16th Street, NW, Washington, DC 20036 (202-872-4600; 800-227-5558)

C&EN Supplements Management

Kevin A. Davies,
Publisher, C&EN

Rudy M. Baum,
Editor-in-Chief (acting), C&EN

Kenneth M. Carroll,
Director, Advertising Sales, C&EN

Dean Baldwin,
Regional Sales Manager, C&EN

Stephanie Holland,
C&EN Marketing Manager

Renee Zerby,
Manager, Composition Production

Joseph B. Davis, Jr.,
Senior Digital Production Associate

Krystal E. King,
Senior Digital Production Associate

Richard C. Smith,
Digital Production Associate

ACS Management

Madeleine Jacobs,
CEO & Executive Director

Brian D. Crawford,
President, ACS Publications

To advertise in Media Group products, contact the Advertising Sales Group at 610-964-8061 or go to CENMediaKit.org.

PUBLISHER'S NOTE

Supplemental Information

IT GIVES ME great pleasure to introduce the second in the series of special supplements being produced every quarter by the C&EN Media Group in 2014.

This C&EN Supplement is devoted to "Advances in Spectroscopy and Materials Science." As with the successful debut edition that we published in March, we are grateful to the many organizations and instrumentation companies that have decided to support this supplement by contributing technical application notes. We are pleased to include titles and abstracts from 10 of the most popular and cited research articles relevant to these themes from the peer-reviewed journal Analytical Chemistry, published (as is C&EN) by the American Chemical Society.

Special thanks go to contributing editor Malorye Allison Branca, who managed the editorial process for this edition; the production team at C&EN for their expert assistance in producing this supplement; and *Analytical Chemistry* managing editor Antonella Mazur and her colleagues.

For our next C&EN Supplement, in September, we are beginning to assemble a report on the *"Top 50 Drugs."* This will be an in-depth report on the stories and takeaways of the most successful and innovative drugs that are both on the market and in the pharmaceutical pipeline.

If you have any thoughts on this supplement or suggestions for future topics or areas we might explore, please get in touch with us.

Kevin Davies, PhD
Publisher, C&EN

The editorial content in this supplement was created without direct involvement of C&EN reporters or editors.

WELCOME TO our latest special supplement to *C&EN,* part of an exciting new series of reports that are complementary to *Chemical & Engineering News* magazine. In this issue, we focus on another pivotal and vibrant field—spectroscopy and materials analysis. The technical and application notes contained in this issue involve materials, pharmaceuticals, food and energy. In these notes, researchers from some of the world's leading companies describe applications for a wide range of important techniques including FTIR, Raman, and NMR.

In addition, we turned to *Analytical Chemistry* to see which reports of the last year were the most popular according to the publication's editors. See their top picks below and find out if you agree with us, or visit http://pubs.acs.org/journal/ancham to make your own picks and view the most recent reports. ■

Malorye Allison Branca
contributing editor,
C&EN Media Group

TOP TEN SPECTROSCOPY AND MATERIAL SCIENCE PAPERS

Analytical Chemistry's Most Popular Papers of the Last Year

Quantitative Vibrational Imaging by Hyperspectral Stimulated Raman Scattering Microscopy and Multivariate Curve Resolution Analysis

Delong Zhang †, Ping Wang ‡, Mikhail N. Slipchenko ‡, Dor Ben-Amotz †, Andrew M. Weiner §, and Ji-Xin Cheng †‡
† Department of Chemistry,
‡ Weldon School of Biomedical Engineering, and
§ Electrical and Computer Engineering, Purdue University, West Lafayette, Indiana 47907, United States
Anal. Chem., **2013,** *85* (1), 98-106
DOI: 10.1021/ac3019119

Spectroscopic imaging has been an increasingly critical approach for unveiling specific molecules in biological environments. Toward this goal, we demonstrate hyperspectral stimulated Raman loss (SRL) imaging by intrapulse spectral scanning through a femtosecond pulse shaper. The hyperspectral stack of SRL images is further analyzed by a multivariate curve resolution (MCR) method to reconstruct quantitative concentration images for each individual component and retrieve the corresponding vibrational Raman spectra. Using these methods, we demonstrate quantitative mapping of dimethyl sulfoxide concentration in aqueous solutions and in fat tissue. Moreover, MCR is performed on SRL images of breast cancer cells to generate maps of principal chemical components along with their respective vibrational spectra. These results show the great capability and potential of hyperspectral SRL microscopy for quantitative imaging of complicated biomolecule mixtures through resolving overlapped Raman bands. ■

Portable, Quantitative Detection of *Bacillus* Bacterial Spores Using Surface-Enhanced Raman Scattering

David P. Cowcher, Yun Xu, and Royston Goodacre
School of Chemistry and Manchester Institute of Biotechnology, University of Manchester, 131 Princess Street, Manchester, M1

7DN United Kingdom
Anal. Chem., **2013,** *85* (6), 3297-3302
DOI: 10.1021/ac303657k

Portable rapid detection of pathogenic bacteria such as *Bacillus* is highly desirable for safety in food manufacture and under the current heightened risk of biological terrorism. Surface-enhanced Raman scattering (SERS) is becoming the preferred analytical technique for bacterial detection, due to its speed of analysis and high sensitivity. However in seeking methods offering the lowest limits of detection, the current research has tended toward highly confocal, microscopy-based analysis, which requires somewhat bulky instrumentation and precisely synthesized SERS substrates. By contrast, in this study we have improved SERS for bacterial analyses using silver colloidal substrates, which are easily and cheaply synthesized in bulk, and which we shall demonstrate permit analysis using portable instrumentation. All analyses were conducted in triplicate to assess the reproducibility of this approach, which was excellent. We demonstrate that SERS is able to detect and quantify rapidly the dipicolinate (DPA) biomarker for *Bacillus* spores at 5 ppb (29.9 nM) levels which are significantly lower than those previously reported for SERS and well below the infective dose of 10^4B. *anthracis* cells for inhalation anthrax. Finally we show the potential of multivariate data analysis to improve detection levels in complex DPA extracts from viable spores. ■

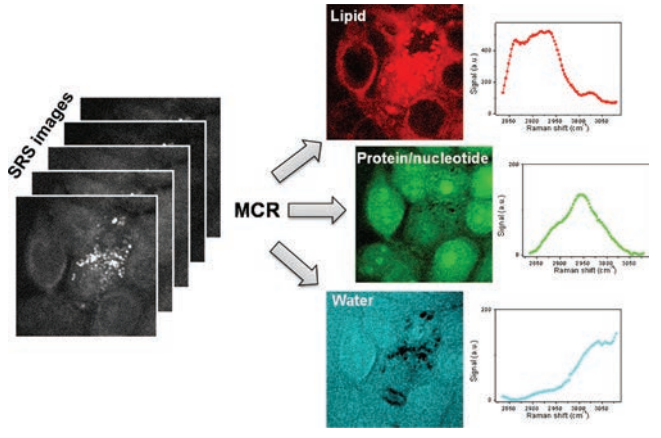

Plasmonic Nanorice Antenna on Triangle Nanoarray for Surface-Enhanced Raman Scattering Detection of Hepatitis B Virus DNA

Ming Li †, Scott K. Cushing †‡, Hongyan Liang §, Savan Suri †, Dongling Ma §, and Nianqiang Wu †
† Department of Mechanical and Aerospace Engineering and ‡ Department of Physics, West Virginia University, Morgantown, West Virginia 26506-6106, United States
§ Institut National de la Recherche Scientifique, INRS-Énergie, Matériaux et Télécommunications, 1650 Boulevard Lionel-Boulet, Varennes, Québec J3X 1S2, Canada
Anal. Chem., **2013,** *85* (4), 2072-2078
DOI: 10.1021/ac303387a

The sensitivity and the limit of detection of Raman sensors are limited by the extremely small scattering cross section of Raman labels. Silver nanorice antennae are coupled with a patterned gold triangle nanoarray chip to create spatially broadened plasmonic "hot spots", which enables a large density of Raman labels to experience strong local electromagnetic field. Finite difference time domain simulations have confirmed that the quasi-periodic structure increases the intensity and the area of the surface plasmon resonance (SPR), which enhances the surface-enhanced Raman scattering (SERS) signal significantly. The SERS signal of the nanorice/DNA/nanoarray chip is compared with that of the nanorice/DNA/film chip. The SERS signal is greatly enhanced when the Ag nanorices are coupled to the periodic Au nanoarray instead of the planar film chip. The resulting spatially broadened SPR field enables the SERS biosensor with a limit of detection of 50 aM toward hepatitis B virus DNA with the capability of discriminating a single-base mutant of DNA. This sensing platform can be extended to detect other chemical species and biomolecules such as proteins and small molecules. ■

Multifunctional Analytical Platform on a Paper Strip: Separation, Preconcentration, and Subattomolar Detection

Abdennour Abbas †, Andrew Brimer †, Joseph M. Slocik ‡, Limei Tian †, Rajesh R. Naik ‡, and Srikanth Singamaneni †
† Department of Mechanical Engineering and Materials Science, Washington University in St. Louis, St. Louis, Missouri 63130, United States
‡ Soft Matter Materials Branch, Materials and Manufacturing Directorate, Wright Patterson Air Force Base, Dayton, Ohio 45433, United States
Anal. Chem., **2013,** *85* (8), 3977-3983
DOI: 10.1021/ac303567g

We report a plasmonic paper-based analytical platform with functional versatility and subattomolar ($<10^{-18}$ M) detection limit using surface-enhanced Raman scattering as a transduction method. The microfluidic paper-based analytical device (μPAD) is made with a lithography-free process by a simple cut and drop method. Complex samples are separated by a surface chemical gradient created by differential

polyelectrolyte coating of the paper. The μPAD with a starlike shape is designed to enable liquid handling by lateral flow without microchannel patterning. This design generates a rapid capillary-driven flow capable of dragging liquid samples as well as gold nanorods into a single cellulose microfiber, thereby providing an extremely preconcentrated and optically active detection spot. ■

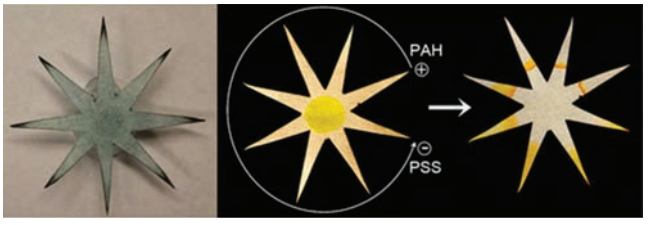

Interfacing Droplet Microfluidics with Matrix-Assisted Laser Desorption/Ionization Mass Spectrometry: Label-Free Content Analysis of Single Droplets

Simon K. Küster †, Stephan R. Fagerer †, Pascal E. Verboket †, Klaus Eyer †, Konstantins Jefimovs ‡, Renato Zenobi †, and Petra S. Dittrich †

† Department of Chemistry and Applied Biosciences, ETH Zürich, Wolfgang-Pauli-Strasse 10, 8093 Zürich, Switzerland

‡ Laboratory for Electronics/Metrology/Reliability EMPA, Swiss Federal Laboratories for Material Science and Technology, Überlandstrasse 129, 8600 Dübendorf, Switzerland

Anal. Chem., **2013,** *85* (3), 1285–1289

DOI: 10.1021/ac3033189

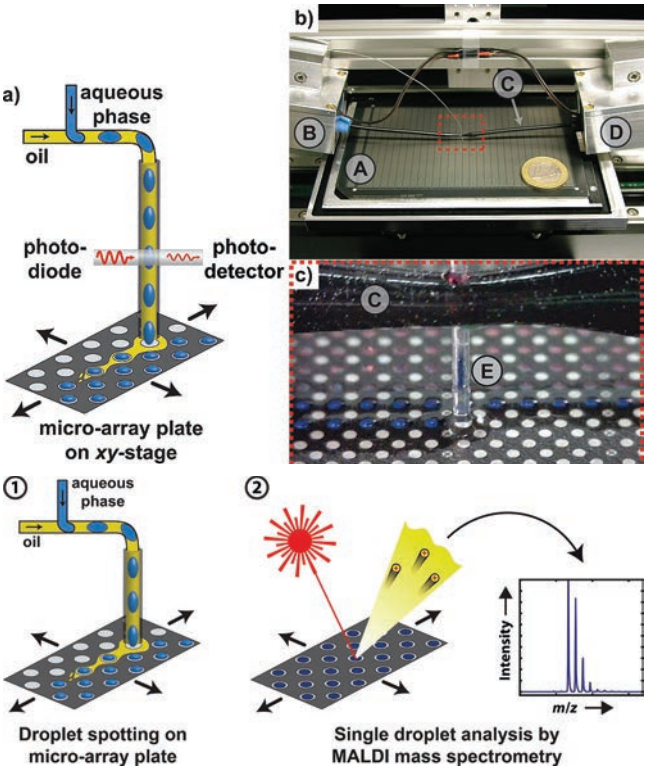

Droplet-based microfluidic systems have become a very powerful tool to miniaturize chemical and biological reactions. However, droplet content analysis remains challenging and relies almost exclusively on optical methods such as fluorescence spectroscopy. Hence, labeling of the analyte is typically required which impedes a more universal applicability of microdroplets. Here we present a novel interface coupling droplet microfluidics and matrix-assisted laser desorption/ionization (MALDI) mass spectrometry for label-free content analysis of single droplets. Nanoliter aqueous droplets immersed in perfluorinated oil are created in a microfluidic T-junction, transferred into a capillary, and deposited on a high-density microarray MALDI plate mounted on a motorized xy-stage. The fully automated system is robust and reliable due to two unique features. First, a simple optical droplet detection system is used to synchronize stage movement and exit of droplets from the capillary. Second, the microarray plate contains an array of over 26 000 hydrophilic spots within a hydrophobic coating, each spot acting as a recipient to confine the droplets and to prevent cross-contamination. The MALDI matrix can also be applied using our system by spotting matrix droplets on the microarray in a separate run. To demonstrate the potential of our system, we studied the enzymatic cleavage of angiotensin I by angiotensin converting enzyme and monitored the increasing concentration of the product angiotensin II over time. The interface provides a robust and fully automated method for rapid label-free and information-rich content analysis of single droplets. With the high number of droplets per plate, this method is particularly suitable for high-throughput screening applications. ■

Fabrication and Characterization of Dual Function Nanoscale pH-Scanning Ion Conductance Microscopy (SICM) Probes for High Resolution pH Mapping

Binoy Paulose Nadappuram, Kim McKelvey, Rehab Al Botros, Alex W. Colburn, and Patrick R. Unwin

Department of Chemistry, University of Warwick, Coventry CV4 7AL, U.K.

Anal. Chem., **2013,** *85* (17), 8070–8074

DOI: 10.1021/ac401883n

The easy fabrication and use of nanoscale dual function pH-scanning ion conductance microscopy (SICM) probes is reported. These probes incorporate an iridium oxide coated

carbon electrode for pH measurement and an SICM barrel for distance control, enabling simultaneous pH and topography mapping. These pH-SICM probes were fabricated rapidly from laser pulled theta quartz pipets, with the pH electrode prepared by in situ carbon filling of one of the barrels by the pyrolytic decomposition of butane, followed by electrodeposition of a thin layer of hydrous iridium oxide. The other barrel was filled with an electrolyte solution and Ag/AgCl electrode as part of a conductance cell for SICM. The fabricated probes, with pH and SICM sensing elements typically on the 100 nm scale, were characterized by scanning electron microscopy, energy-dispersive X-ray spectroscopy, and various electrochemical measurements. They showed a linear super-Nernstian pH response over a range of pH (pH 2–10). The capability of the pH-SICM probe was demonstrated by detecting both pH and topographical changes during the dissolution of a calcite microcrystal in aqueous solution. This system illustrates the quantitative nature of pH-SICM imaging, because the dissolution process changes the crystal height and interfacial pH (compared to bulk), and each is sensitive to the rate. Both measurements reveal similar dissolution rates, which are in agreement with previously reported literature values measured by classical bulk methods. ■

SERS Primers and Their Mode of Action for Pathogen DNA Detection

Danny van Lierop, Iain A. Larmour, Karen Faulds, and Duncan Graham
Centre for Molecular Nanometrology, WestCHEM, Pure and Applied Chemistry, University of Strathclyde, 295 Cathedral Street, Glasgow G1 1XL, United Kingdom
Anal. Chem., **2013,** *85* (3), 1408–1414
DOI: 10.1021/ac302254h

SERS primers have been used to directly detect specific PCR products utilizing the difference in adsorption of single-stranded and double-stranded DNA onto nanoparticle surfaces. Herein, seven parameters important for improved positive SERS assays for real applications were investigated. First, we applied a model system for optimization experiments, followed by a PCR assay to detect pathogen DNA, and then the introduction of a new assay that utilizes the 5′→3′ exonuclease activity of *Taq* DNA polymerase to partly digest the SERS probe, generating dye-labeled single-stranded DNA increasing the SERS signals for detection of pathogen DNA. Applying the model system, it was found that uni-molecular SERS primers perform better than bi-molecular SERS primers. However, within the PCR assays, it was found that uni- and bi-molecular SERS primers performed very similarly, and the most reproducible results were obtained using the 5′→3′ exonuclease digestion assay. These SERS-based assays offer new routes over conventional fluorescence-based techniques without compromising sensitivity or selectivity. ■

Breath Analysis with Broadly Tunable Quantum Cascade Lasers

Katharina Wörle †, Felicia Seichter †, Andreas Wilk †, Chris Armacost ‡, Tim Day ‡, Matthias Godejohann §, Ulrich Wachter, Josef Vogt, Peter Radermacher, and Boris Mizaikoff †
† Institute of Analytical and Bioanalytical Chemistry, University of Ulm, 89081 Ulm, Germany
‡ Daylight Solutions Inc., San Diego, California 92128, United States
§ MG Optical Solutions GmbH, 86922 Eresing, Germany Klinik für Anästhesiologie, Sektion Anästhesiologische Pathophysiologie und Verfahrensentwicklung, Universitätsklinikum Ulm, 89081 Ulm, Germany
Anal. Chem., **2013,** *85* (5), 2697–2702
DOI: 10.1021/ac3030703

With the availability of broadly tunable external cavity quantum cascade lasers (EC-QCLs), particularly bright mid-infrared (MIR; 3–20 μm) light sources are available offering high spectral brightness along with an analytically relevant spectral tuning range of >2 μm. Accurate isotope ratio determination of $^{12}CO_2$ and $^{13}CO_2$ in exhaled breath is of critical importance in the field of breath analysis, which may be addressed via measurements in the MIR spectral regime. Here, we combine for the first time an EC-QCL tunable across the $^{12}CO_2/^{13}CO_2$ spectral band with a miniaturized hollow waveguide gas cell for quantitatively determining the $^{12}CO_2/^{13}CO_2$ ratio within the exhaled breath of mice. Due to partially overlapping spectral features, these studies are augmented by appropriate multivariate data evaluation and calibration techniques based on partial least-squares regression along with optimized data preprocessing. Highly accurate determinations of the isotope ratio within breath samples collected from a mouse intensive care unit validated via hyphenated gas chromatography–mass spectrometry confirm the viability of IR-HWG-EC-QCL sensing techniques for isotope-selective exhaled breath analysis. ■

High-Resolution Quantitative Metabolome Analysis of Urine by Automated Flow Injection NMR

Laeticia Da Silva †, Markus Godejohann ‡, François-Pierre J. Martin †, Sebastiano Collino †, Alexander Bürkle §, María Moreno-Villanueva §, Jürgen Bernhardt, Olivier Toussaint, Beatrix Grubeck-Loebenstein #, Efstathios S. Gonos, Ewa Sikora, Tilman Grune, Nicolle Breusing, Claudio Franceschi ¶, Antti Hervonen ▼, Manfred Spraul ‡, and Sofia Moco †
† BioAnalytical Science, Nestle Research Center, Vers-chez-les-Blanc, P.O. Box 44, 1000 Lausanne 26, Switzerland
‡ Bruker-Biospin GmbH, Am Silberstreifen 4, D-76287 Rhein-

stetten, Germany
§ Molecular Toxicology Group, Department of Biology, University of Konstanz, 78457 Konstanz, Germany BioTeSys GmbH, 73728 Esslingen, Germany Research Unit on Cellular Biology (URBC), University of Namur (FUNDP), 5000 Namur, Belgium
# Institute for Biomedical Aging Research, University of Innsbruck, 6020 Innsbruck, Austria Institute of Biological Research and Biotechnology, National Hellenic Research Foundation, Athens 11635, Greece Nencki Institute of Experimental Biology, 02-093 Warsaw, Poland Institute of Biological Chemistry and Nutrition, University of Hohenheim, 70593 Stuttgart, Germany
¶ Department of Experimental Pathology, University of Bologna, 40126 Bologna, Italy
School of Public Health, University of Tampere, 33014 Tampere, Finland
Anal. Chem., **2013,** *85* (12), 5801–5809
DOI: 10.1021/ac4004776

Metabolism is essential to understand human health. To characterize human metabolism, a high-resolution read-out of the metabolic status under various physiological conditions, either in health or disease, is needed. Metabolomics offers an unprecedented approach for generating system-specific biochemical definitions of a human phenotype through the capture of a variety of metabolites in a single measurement. The emergence of large cohorts in clinical studies increases the demand of technologies able to analyze a large number of measurements, in an automated fashion, in the most robust way. NMR is an established metabolomics tool for obtaining metabolic phenotypes. Here, we describe the analysis of NMR-based urinary profiles for metabolic studies, challenged to a large human study (3007 samples). This method includes the acquisition of nuclear Overhauser effect spectroscopy one-dimensional and *J*-resolved two-dimensional (*J*-Res-2D) ^{1}H NMR spectra obtained on a 600 MHz spectrometer, equipped with a 120 μL flow probe, coupled to a flow-injection analysis system, in full automation under the control of a sampler manager. Samples were acquired at a throughput of 20 (or 40 when *J*-Res-2D is included) min/sample. The associated technical analysis error over the full series of analysis is 12%, which demonstrates the robustness of the method. With the aim to describe an overall metabolomics workflow, the quantification of 36 metabolites, mainly related to central carbon metabolism and gut microbial host cometabolism, was obtained, as well as multivariate data analysis of the full spectral profiles. The metabolic read-outs generated using our analytical workflow can therefore be considered for further pathway modeling and/or biological interpretation. ■

Direct Analysis of Textile Fabrics and Dyes Using Infrared Matrix-Assisted Laser Desorption Electrospray Ionization Mass Spectrometry

Kristin H. Cochran †, Jeremy A. Barry †, David C. Muddiman †, and David Hinks ‡
† W.M. Keck FT-ICR Mass Spectrometry Laboratory, Department of Chemistry, North Carolina State University, Raleigh, North Carolina 27695, United States
‡ Department of Textile Engineering, Chemistry, and Science, North Carolina State University, Raleigh, North Carolina 27695, United States
Anal. Chem., **2013,** *85* (2), 831–836
DOI: 10.1021/ac302519n

The forensic analysis of textile fibers uses a variety of techniques from microscopy to spectroscopy. One such technique that is often used to identify the dye(s) within the fiber is mass spectrometry (MS). In the traditional MS method, the dye must be extracted from the fabric and the dye components are separated by chromatography prior to mass spectrometric analysis. Direct analysis of the dye from the fabric allows the omission of the lengthy sample preparation involved in extraction, thereby significantly reducing the overall analysis time. Herein, a direct analysis of dyed textile fabric was performed using the infrared matrix-assisted laser desorption electrospray ionization (IR-MALDESI) source for MS. In MALDESI, an IR laser with wavelength tuned to 2.94 μm is used to desorb the dye from the fabric sample with the aid of water as the matrix. The desorbed dye molecules are then postionized by electrospray ionization (ESI). A variety of dye classes were analyzed from various fabrics with little to no sample preparation allowing for the identification of the dye mass and in some cases the fiber polymer. Those dyes that were not detected using MALDESI were also not observed by direct infusion ESI of the dye standard. ■

CHARACTERIZATION OF ALUMINUM ALLOY DEPOSITION DURING AUTOMOTIVE WHEEL COATING

Yvette Mattley, Ph.D. Ocean Optics, Inc.

Abstract

In this application note, we evaluated the change in reflectance that occurred with the direct current sputtering of a thin film of aluminum chrome alloy on a cured, powder-coated wheel. The objective of the measurements was to investigate the change in reflection as a function of deposition time, both before and after clear coating with an acrylic powder for UV protection.

Introduction

Reflectance measurements express the amount of light reflected from a surface as a percentage of the light used for illumination. Light reflection varies based on the texture of the surface. Very smooth surfaces like mirrors exhibit specular reflection, in which all rays in the incident beam reflect in the same direction (angle of reflection = angle of incidence). Rough or matte surfaces exhibit diffuse reflection, in which the rays of the incident beam are scattered in all directions. The typical surface is in-between, having both specular and diffuse components.

Methods/Conditions

Using the high reflectivity reference standard as our reference, we measured the specular reflection of a common location on the spoke of each sample wheel. Samples 1, 3 and 5 (see Fig. 1) were coated with an acrylic powder to provide UV protection. Alloy deposition times varied from 30–90 seconds. Samples 1 and 2 were coated for 30 seconds, samples 3 and 4 were coated for 60 seconds and samples 5 and 6 were coated for 90 seconds.

Measurements were made using a modular spectroscopy setup including a USB4000-UV-VIS spectrometer (200-850 nm), a balanced deuterium-halogen light source and a premium-grade 400 μm solarization resistant reflection probe. The reflection spectra measured for the wheel samples with and without UV protective coating after 30, 60 or 90 second deposition times are shown in the figure.

Results

The shape and intensity of the reflection spectra measured for the wheel samples correlated with both the deposition time and presence of UV protective coating. The reflected intensity of the peaks between 300-400 nm (for samples 2, 4 and 6 without UV coating) and for the peak at 510 nm (for all the samples) increased with deposition time as more of the shiny aluminum alloy was deposited on the sample surface. The presence of the UV coating on samples 1, 3 and 5 was evidenced by lower reflectance in the UV region for these samples due to absorbance of UV light by the UV protective coating.

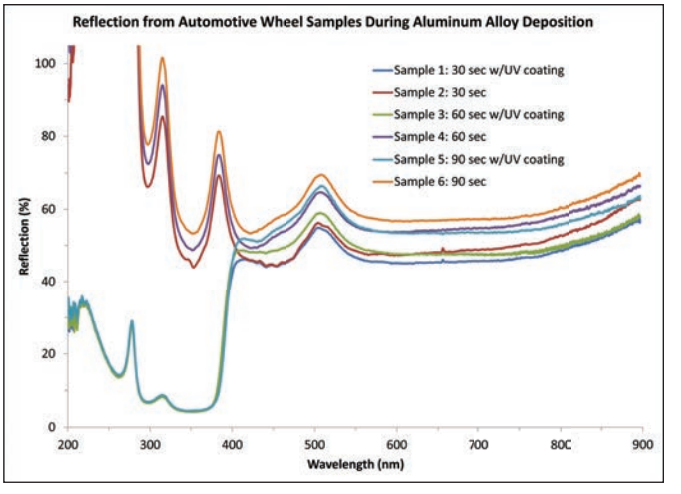

Figure 1

Specular reflection from automotive wheel samples during the deposition of an aluminum alloy correlates with the deposition time and presence or absence of a UV protective coating.

Conclusions

As we have demonstrated, reflectance measurements are useful for detecting changes in the surface of an automotive wheel sample as an alloy or UV protective coating is deposited on its surface. Similar modular spectroscopy measurements could be exploited by researchers, QC professionals and others for the qualitative and quantitative characterization of surface coatings and thin film deposits. This type of measurement could also be made for the sorting, quality control and scientific study of samples as diverse as automotive parts, paint, coffee beans and lizards. ■

Ocean Optics, Inc.
830 Douglas Avenue
Dunedin, FL 34698
Tel: (727)-733-2447
Email: info@oceanoptics.com
Website: www.oceanoptics.com

DEMONSTRATED ACCURACY OF THE BECKMAN COULTER LS SERIES

Beckman Coulter Life Sciences

Introduction

The Beckman Coulter LS Series laser diffraction instruments incorporate two enhancements to basic light scattering technology: resolution across the range is greatly increased by using greater numbers of detectors per unit angle than other similar instruments, and measurements of particles smaller than 0.5 micron are substantially improved by a patented technology called polarization intensity differential scattering (PIDS). These two enhancements make the Beckman Coulter LS Series design extremely accurate and reliable.

The PIDS technology uses three wavelengths of light, filtered for polarization in the vertical and horizontal planes. Six detectors (in addition to the 126 detectors used for measuring scattered laser light) are positioned at around 90 degrees to the direction of the light path to measure the differential intensity between scattered light of vertical and horizontal polarizations. Thus, the total number of measurements in a single test is 166: 126 scattering detectors and in PIDS, a total of 36 measurements are made at six scattering angles and three wavelengths, each at two polarizations.

The combination of multiple wavelengths and two polarizations provides information that differentiates between submicron particle sizes and dramatically increases resolution. Although PIDS uses a second light source split into six types, the scattering of these light beams by particles is described by the same Mie theory, so all scattering information is converted to particle size using the same algorithm in a single operation. The resolution and accuracy of PIDS was tested using a mixture of particle sizes in the submicron region.

Methods/Conditions

Here, the accuracy of the LS Series is demonstrated by measuring a variety of reference materials. All materials used were spherical to avoid any shape-dependent bias. A series of nine NIST-traceable microspheres from Duke Scientific (now ThermoFisher) were measured. Eight of these consisted of polystyrene latex spheres (either pure polystyrene, PSL or polystyrene divinylbenzene, PSDL) and one consisted of glass spheres (GS). All of the NIST-traceable materials have very narrow particle size distributions. In addition, SRM 1003b, a broad distribution of glass beads from NIST, was measured.

Two of the NIST-traceable materials were selected to test the accuracy of the volume percentage recovery of the instrument by mixing various proportions of the two materials. If an instrument does not correctly recover volume percentages, then little confidence can be placed in results that indicate the presence of secondary populations of particles that can have important consequences for the performance of a material.

The two materials chosen for this part of the evaluation were selected using two criteria: that their diameters were relatively close together, allowing a simultaneous test of resolution, and that they were packaged dry, allowing accurate determination of concentration by weight. Finally, submicron resolution and the ability to recover correct volume percents for a mixture of submicron particles were tested using a trimodal mixture of NIST-traceable particles from Duke Scientific.

Results

Table 1 lists the results for the NIST traceable samples analyzed by the laser diffraction instrument individually. Since the certified mean diameters are uncertain by a specified quantity, any results within the uncertainty limits are listed as 'in' for in-specification in Table 1. The error for results that fall outside the uncertainty limits is calculated from the nearest uncertainty limit. Of the nine materials, the LS series recovered mean diameters with the uncertainty limits for seven. The recovered mean for the 1.034-micron polystyrene spheres was 2.37% outside the lower uncertainty limit, and the recovered mean for the 274-micron polystyrene divinylbenzene spheres was 1.62% outside the upper uncertainty limit. Overall, results emphasize the effectiveness of the Beckman Coulter LS Series instrument to measure particle size accurately.

Table 1: The LS Series Results for NIST Traceable Samples

	Traceable Diameter		LD Result	
Materials	d(μm)	+(μm)	d(μm)	in/out
304nm PSL	0.304	0.006	0.306	in
503nm PSL	0.503	0.004	0.506	in
1μm PSL	1.034	0.020	0.99	2.37%
10μm PSDL	10.0	0.3	10.14	in
40μm GS	40.0	2.8	41.52	in
116μm PSDL	116.0	2.3	116.8	in
167μm PSDL	167.0	3.4	167.8	in
274μm PSDL	274.0	5.5	284.1	1.62%
539μm PSDL	539.0	11.0	550.0	in

Table 2 lists the results for the volume- percent-recovery test using three mixtures of 167-micron and 274-micron

spheres, indicated in the first column for the approximate ratio of 167 μm:274 μm PSDL. The second column lists the actual volume percentage of 167 μm PSDL added the LS Series recovered within 2% (as a percentage of the total volume) of the added volume percentages (the third column), which indicates that the LS Series has excellent resolution for an instrument of this type given that the ratio of the mean diameters is only 1.64.

Table 2: Information Recovered of Mixtures of PSDL

	Added	Recovered		
Ratio	V_{167}%	V_{167}%	$d_{167}(\mu m)$	$d_{274}(\mu m)$
1:1	50.35	51.50	166.8	283.6
2:1	66.57	68.55	168.6	282.8
1:3	25.0	23.67	166.7	279.1

The right two columns are the mean sizes recovered from the particle size distribution peaks.

The mean particle diameter and the uncertainty limits of the NIST SRM 1003b material were calculated from the certified cumulative-percent-less-than values, the upper and lower limits of the certified values. Table 3 shows that the mean diameter and standard deviation are within those calculated for the upper and lower limits, and deviate from those of the certified values only 1.3% for the mean and 0.9% for the standard deviation.

Table 3: Particle Size Distribution of NIST SRM 1003b

	Calculated from Certified Values			LD
Parameter	Lower limit	Mean	Upper Limit	Mean
d(μm)	36.53	37.09	37.66	37.59
SD(μm)	8.953	9.048	9.112	8.967

Table 4 lists results for the submicron trimodal mixture, including the recovered means and volume percentages for the three modes. While still superior in competitive performance, the accuracy for complex samples is not as high in the submicron region as it is for larger particles. The recovered volume percentages are skewed towards the 83-nm component and the two smaller components show errors in mean diameter that are larger than any errors found for single mode standards. The mean diameter of the 503-nm component was recovered without error.

Table 4: Results for Submicron Trimodal Mixture

$d_{certified}$ (nm)/V%	d_{LD} (nm)	$V\%_{LD}$
83±2.7(nm)/50%	74	55
204±6(nm)/25%	218	24
503±4(nm)/25%	504	21

Conclusion

Most laser diffraction instruments are not able to distinguish the separate modes in submicron samples such as these, but the PIDS permits successful analysis of complex submicron distributions. The performance of the Beckman Coulter LS Series relative to traceable standards indicates the instrument can be used with confidence, and that eh particle size distributions it produces accurately reflect the sample material. ■

BECKMAN COULTER Life Sciences

Beckman Coulter Life Sciences
Particle Counting and Characterization
481 California Ave.
Grants Pass, OR 97526
Tel: (541) 472-6508
Website: www.particle.com

Particle Monitoring for Industrial Applications

*Increase process throughput and quality; ensure your catalyst, resins, and polymer materials are in specification with the **LS 13 320.***

The Beckman Coulter LS 13 320 offers:

- Fast – automated cleaning and background routines ensure sample to sample carryover is minimized
- Stop using a sieve and simply use the LS 13 320 sieve analysis function to compare both new and historical data
- Easily set up and save test methods for any chemical or material for quick access on common samples used frequently
- Reproducible and accurate data is assured with the LS 13 320 with powerful unique optical design
- Run samples in either aqueous, solvent or dry mode with auto-docking LS 13 320 sample modules

Not all laser diffraction instruments are created equal!

Learn how the Beckman Coulter LS series can increase your confidence in particle size data!

---

*The **HIAC 8011+** ensures cleanliness of your fluids and ends costly downtime!*

- False counts can create downtime and drive unnecessary production costs
- Sample management system ensures consistent, accurate data
- One button sampling - results under 60 seconds | Quickly load up to 20 custom test recipes | Setup your own sampling recipe in less than 5 steps
- Eliminate printing and go paperless. Get the data immediately in a PDF or Excel® file

The HIAC™ 8011+ Liquid Particle Counting System, is the culmination of over 30 years of particle counting expertise. Designed for ease of use, one button sampling yields results in under 60 seconds.

Visit **www.particle.com** for additional information

BECKMAN COULTER Life Sciences

DEPTH PROFILING OF POLYMER LAMINATES USING CONFOCAL RAMAN MICROSCOPY

Peng Wang, Ph.D. and Thomas J. Tague, Jr., Ph.D. Bruker Optics

Abstract

Confocal Raman microscopy was used to study multilayer polymer laminate samples. The confocal capability was demonstrated by resolving four layers as well as a mirror image that results with the addition of a metal substrate.

Methods/Conditions

Raman spectroscopy is based on the inelastic scattering of monochromatic light when the frequency of photons changes upon interaction with a sample. Such frequency shifts represent the vibrational and rotational energies of molecular bonds as well as molecular structures and therefore can be used for molecular and morphological identification. As such, Raman spectroscopy has found its applications in multiple areas including industry and academic research. Another superb feature associated with this technique is the achievable spatial resolution when using Raman microscopy. In particular, depth profiling using confocal Raman microscopy has assured its wide-spread proliferation into more areas. By moving the laser focus in the z-direction either a complete 2D or even 3D depth profile of a structured sample can be generated. In this study, a multilayer polymer laminate was investigated. An innovative result was observed in existence of a metal layer.

A Bruker Senterra Raman microscope was equipped with three excitation lasers (532 nm, 633 nm, 785 nm) and a computer controlled xyz stage allowing increment stepping down to 0.1.m in all directions. The confocal design of the Raman microscope minimizes out-of-focus contributions from unwanted spectral information by optical sectioning the z-direction with confocal pinholes. A multilayer laminated packaging material containing a metal foil layer was studied. A 50x objective was used in combination with the 785 nm laser. The depth profile was recorded over a range of 0-120 microns with a step size of 2 microns and is shown in Fig. 1. The depth profiling result on the laminate containing a metal foil (Fig. 1a) shows a rather symmetric layer combination. Representative spectra of all layers are shown in Fig. 1c. The layers have been identified via library searching using Bruker's OPUS spectroscopy software. Starting from the surface, the layers as identified are polyethylene (PE), nylon, polyethylene (PE), poly (ethylene terephthalate) (PET), polyethylene (PE), nylon, and polyethylene (PE). The thicknesses are estimated to be 20μm, 10μm, 20μm, 15μm, 20μm, 10μm and 20μm respectively. However, after the metal foil was peeled off, depth profiling over a similar range indicated the presence of only four layers as shown in Fig. 1b (PE, nylon, PE and PET). It turns out that the extra layers indicated in Fig. 1a are mirror images introduced by the metal foil.

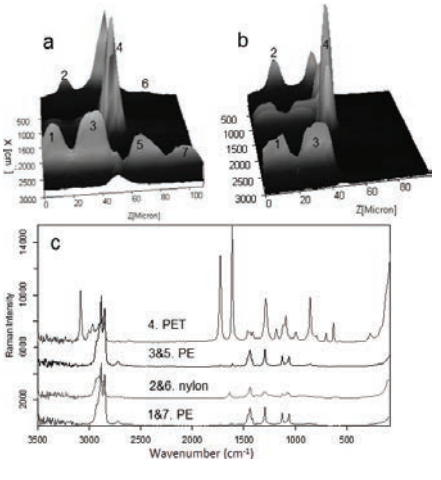

Figure 1

a *3D depth profiling plot of the multilayer laminate containing a metal foil,* ***b*** *3D depth profiling plot of the multilayer laminate after peeling off the metal foil,* ***c*** *representative Raman spectra of each layer.*

Results

The results demonstrate the usefulness of confocal Raman microscopy for the investigation of multilayer polymer films without the need to perform cross-section analysis. Not only are 3500 individual layers well resolved and identified, but the thickness is also determined. Most interestingly, when a metal layer exists, the laser light will be reflected and refocused into a layer above the metal and a mirror image of the structure centered by the metal layer is generated. Although the mirror-imaged layers are due to artifacts, the phenomenon unambiguously proves the confocal capability of Raman microscopy. ■

Bruker Optics
Manning Park
19 Fortune Drive
Billerica, MA 01821
Tel: (978) 439-9899
Website: www.bruker.com

LUMOS

FT-IR microscopy made easy

- Stand-alone FT-IR microscope with full automation
- Simple easy-to-use interface
- Motorized ATR crystal
- Automated measurements in transmission, reflection and ATR
- Comprehensive validation with 21 CFR part 11
- 10 year warranty on laser & interferometer
- 5 year warranty on IR source

Bruker's new LUMOS is a fully automated FT-IR microscope with an integrated FT-IR spectrometer. LUMOS is designed to combine highest quality in visible inspection and highest performance in infrared spectral analysis. With motorization and networking of all moveable components, the LUMOS provides an ease of use never before seen in FT-IR microscopy.

Contact us for more details: www.bruker.com/lumos • www.lumos-ir.com

Bruker Optics Inc.
Billerica, MA · USA
Phone +1 (978) 439-9899
Fax +1 (978) 663-9177
E-Mail: info@brukeroptics.com

FT-IR

Innovation with Integrity

FTIR MICROSCOPIC ANALYSIS OF MICRO-PARTICLES

Bruker Optics

Introduction

There are numerous fields of application where the analysis of small particles is of considerable interest (less than 100 microns). Small particles are found frequently as unwanted contaminants in products like pharmaceuticals, food, electronics, or even as air pollutants. They can also occur as a side product being generated from the production of all kinds of formulations like cleaning agents or polymers. In cases where the particles cannot be obtained as bulk material, or when they need be analyzed individually, FTIR microscopy is a powerful technique for determining their chemical identity. With FTIR microscopy, it is possible to collect infrared data from anywhere on a sample with very high spatial resolution making it possible to readily analyze complex multicomponent materials. In fact, one single microscopic particle is enough for a chemical analysis, something that cannot be achieved by most other analytical techniques. Furthermore, FTIR analysis is nondestructive permitting the use of other analytical techniques might be applied afterwards if applicable.

Methods/Conditions

The LUMOS FTIR microscope is an all-in-one solution with an integrated FTIR spectrometer, a high degree of motorization and a dedicated user interface. It also utilizes state-of-the-art optics for optimal sample visualization and infrared data collection. The LUMOS uses a new approach for sample visualization utilizing an 8x Schwartzchild reflecting objective with a variable numerical aperture (NA). Optimal sample visualization is performed with a NA of 0.4 and optimal data collection in ATR, transmission, and reflection modes is accomplished with a NA of 0.6. The innovative highly accurate piezo drive attenuated total reflectance (ATR) acquisition mode performs the complete measurement procedure fully automated including background and sample measurements. To provide perfect contact of the ATR crystal with samples ranging from soft to very hard, contact pressure is monitored precisely and is software selectable. The long working distance and large field-of-view (1.5x1.2 mm) make it very easy to locate and position the sample. Fully automated chemical mapping is readily performed using the dedicated OPUS video wizard, a user interface that always provides the optimal parameters for the desired measurement mode.

A microscopic particle inclusion (see Fig. 1) has a diameter of about 22 μm and is hard to distinguish from the matrix material in the visual image. In order to visualize the particle and to gather information about its chemical nature, a mapping of the inclusion was performed with a 7x7 measurement grid with each grid cell having an aperture setting of 12x12 μm as indicated by the red lines.

Results

The IR spectrum of the particle has a pronounced double band at 1650 and 1550 cm^{-1} that is not present in the surrounding matrix. The particle's corresponding chemical image was created by integrating the characteristic band of the inclusion, which shows much higher contrast between the inclusion and the surrounding matrix than the visual image. In order to reveal the chemical nature of the inclusion a library search was performed on the particle spectrum. The search result clearly shows that the particle is a polyamide. ■

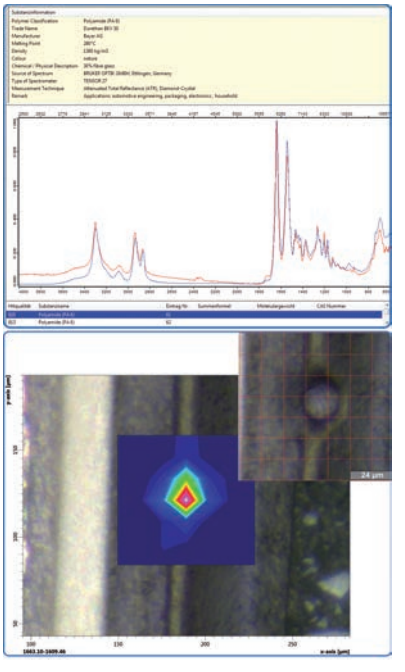

Figure 1

Library search result of sample point located in the center of the map and chemical image of the inclusion overlaid on the visual image (inset: visual image of the inclusion with knife edge aperture positions marked in red).

Bruker Optics
Manning Park
19 Fortune Drive
Billerica, MA 01821
Tel: (978) 439-9899
Website: www.bruker.com

IDENTIFICATION OF A MULTI-COMPONENT CONTAMINANT USING AN ADVANCED CONTAMINANT ANALYSIS PROGRAM

Shimadzu Scientific Instruments

Abstract

This application note introduces the use of an FTIR contaminant analysis program for easy identification of contaminants.

Introduction

Many contaminants often consist of a mixture of substances. A spectrum search for component mixtures typically requires that the search criteria be changed to identify components other than the principle constituent, and this necessitates some degree of expertise in reading spectra. This application note presents a newly designed contaminant analysis program for simple identification of components.

Methods/Conditions

Contaminant Analysis Program: Shimadzu's Contaminant Analysis Program presents a technique that combines spectrum search and peak matching to not only identify the principle constituent, but also indicate the possible existence of sub-constituents from very small characteristic peaks that also appear in the spectrum. Consisting of 553 spectra, it incorporates algorithms that focus on spectral characteristics, rather than performing simple spectrum searches, and allows the automation of the process, including searching, judgment, and report creation.

Analysis of Resin: Various types of additives are added to resin materials to enhance their material properties. The addition of these additives may result in their peaks overlapping those of the resin peaks, thereby complicating and adding a level of difficulty to the analysis. In this analysis of vinyl chloride resin (PVC), measurement was conducted by the single reflection ATR method.

Analytical Conditions:

Instruments:	IRPrestige-21, DuraSamplIR-II
Resolution:	4 cm^{-1}
Accumulation:	45
Apodization:	Happ-Genzel
Detector:	DLATGS

See Fig. 1 for analytic results for resin.

Results

The calibration curve and accuracy (1σ) for each element are shown in Fig. 1

Conclusion

This application introduced an example of the analysis of materials consisting of resin mixtures using the upgraded Contaminant Analysis Program. Resin materials often contain inorganic substances, but these inorganic substances can now be easily detected using the upgraded Contaminant Analysis Program. In cases where even more accurate confirmation of inorganic substances is required, the use of an instrument specifically designed for analysis of inorganic substances, such as an X-ray fluorescence spectrometer, is recommended for validation.

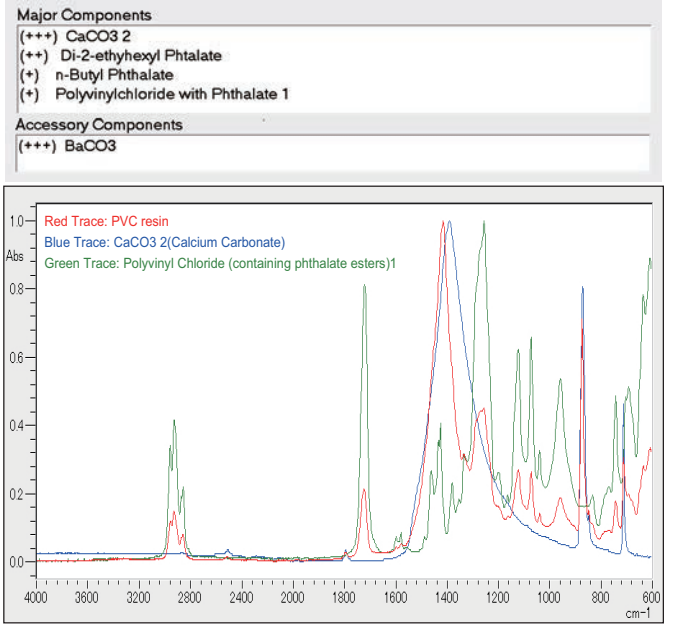

Figure 1

Analytical results for resin, obtained using the Contaminant Analysis Program.

References

1. JIS K 6230 Rubber - Identification - Infrared spectroscopic method. ■

SHIMADZU
Excellence in Science

Shimadzu Scientific Instruments
7102 Riverwood Drive
Columbia, MD 21046
Tel: (410) 381-1227
Website: www.ssi.shimadzu.com

NON-CONTACT MEASUREMENT OF RESIDUAL CURE AND THERMAL EXPANSION OF COATINGS

TA Instruments

Abstract

A new experimental technique is introduced for non-contact dilatometry. This technique is used to measure an epoxy coating that exhibits thermal expansion, residual cure, and a glass transition.

Introduction

The dimensional stability of thin coatings are important to quantify and traditionally difficult to measure. A large mismatch of the coefficient of thermal expansion (CTE) between the coating and substrate can lead to poor adhesion or cracks in the coating. While pushrod-based TMA and dilatometer instruments are commonly used for CTE measurements, coatings often pose practical challenges to these techniques. Sample preparation for thin and brittle coatings can be problematic and even the low contact forces exerted can lead to artifacts in the data.

New non-contact optical methods for dilatometry are well-suited to this irregular sample type. Using the shadowed light method to measure dimension change under controlled temperature, the DIL 806 optical dilatometer is ideal for characterizing thin films and other samples that have size or preparation restrictions. The method is equally effective for opaque, translucent or transparent samples.

Methods/Conditions

Measurements were performed using the DIL 806 non-contact optical dilatometer (TA Instruments, New Castle, DE USA). The test specimen was measured in three heating cycles from ambient to 275 °C at a heating rate of 10 °C/min under an air atmosphere.

The specimen of interest was an epoxy coating from an inner tube wall. The coating was removed manually from the inner tube wall and had a thickness of approximately 350 μm and a specimen length of 18 mm. Measurements were performed parallel to the axial direction of the tube with the freestanding coating supported by a fixture for thin films. Sample preparation requirements are minimal, as the flat and parallel faces that are traditionally required for accurate dilatometry or TMA measurements are unneeded for this optical measurement.

Results

On the first heating cycle (Fig. 1, blue curve) the sample exhibits a CTE of 49×10^{-6} K^{-1} before undergoing contraction beginning at *ca.* 105 °C. This volumetric contraction is consistent with further curing of the epoxy and leads to an overall reduction in length of 1.2%. Second and third heating cycles (Fig. 1, red and black curves) show a glass transition of 121 °C and CTE values below and above the glass transition of 42×10^{-6} K^{-1} and 110×10^{-6} K^{-1}, respectively.

Discussion

The non-contact optical method provides a reliable measurement of the CTE of the coating directly from the manufactured part. The data also reveals that the part as-received was incompletely cured, as demonstrated by the volumetric contraction on the first heating. The non-contact optical method is shown to be an effective, reliable, facile methodology for characterizing coatings and other specimen types that may pose experimental challenges to mechanical techniques. ■

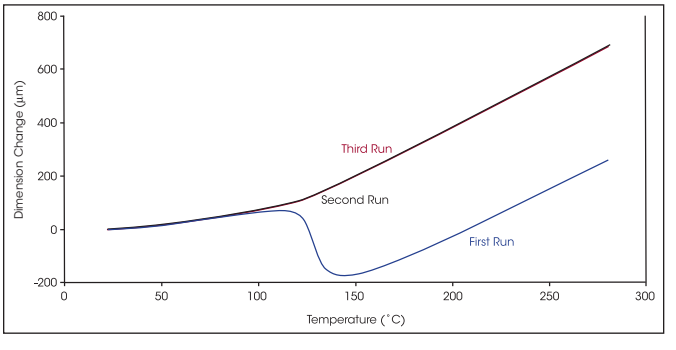

Figure 1

The temperature-dependent dimension change of an epoxy coating in three separate heating cycles. The first heating leads to a contraction of the sample associated with residual curing. On subsequent heatings a constant CTE and a glass transition temperature of 121 °C are observed.

TA Instruments
159 Lukens Drive
New Castle, DE 19720
Tel: (302) 427-4000
Fax: (302) 427-4001
Email: info@tainstruments.com
Website: www.tainstruments.com

The CLEAR CHOICE for
Rubber Rheology

The all new RPA *elite* for advanced rubber rheology features:

- An ultra-rigid frame, transducer, and direct drive motor
- Powerful motor for the highest combination of strain and frequency
- State-of-the-art electronics with advanced Fourier Transform data analysis
- Scarabaeus Software for instrument control and user-friendly data analysis

The RPA *elite* is part of the new line of rubber testing products from TA Instruments and is backed by our world-renowned global direct support network.

TA

www.tainstruments.com

PLASMA MONITORING WITH MODULAR HIGH RESOLUTION SPECTROSCOPY

Yvette Mattley, Ph.D. Ocean Optics, Inc.

Abstract

In this application note, a high resolution modular spectroscopy setup was used to monitor changes in argon plasma emission following the introduction of hydrogen gas to a plasma chamber. The objective was to acquire plasma emission spectra in real time through a window in the plasma chamber for use in monitoring and controlling plasma-based processes.

Introduction

Plasma is used in a range of applications including elemental analysis, film deposition, plasma etching and surface cleaning. Plasma monitoring via the measured emission spectrum can provide detailed elemental analysis for the sample and enable determination of parameters required for controlling a plasma-based process. Parameters like gas mixture, plasma temperature and particle density are all critical for controlling the plasma process. Varying these parameters via introduction of various gases or particles to the plasma chamber will change the plasma characteristics, impacting the interaction of the plasma with the substrate. The ability to monitor and control the plasma in real time leads to improved processes and products.

Methods/Conditions

We used an HR2000+ high resolution spectrometer (200-1100 nm) to measure changes in the emission of an argon plasma as increasing concentrations of hydrogen were introduced to a plasma chamber. Spectral data was acquired for the plasma contained in a closed reaction chamber with the spectrometer, fiber and cosine corrector collecting emission spectra through a small window from outside the chamber.

Results

The spectra measured for argon plasma through the window of the plasma chamber before and after the addition of hydrogen are shown in the figure. The strong spectral lines from 690-900 nm are emission lines from neutral argon (Ar I) with the lower intensity lines from 400-650 nm resulting from the singly ionized argon atoms (Ar II). This spectral information can be used to determine a range of parameters for monitoring and controlling a plasma-based process like thin film deposition or end point detection during semiconductor fabrication.

Hydrogen gas is a secondary gas added to argon plasma to change the properties of the plasma. As shown in Fig. 1, as increasing amounts of hydrogen are added to the chamber, the intensity of the argon lines between 700-900 nm decreases as the hydrogen lines appear between 350-450 nm. These spectra demonstrate the power of modular spectroscopy for measuring plasma emission in real time to monitor the impact of a secondary gas on plasma properties. The spectral changes observed could be used to ensure the optimal amount of secondary gas was added to the chamber to achieve the desired plasma characteristics.

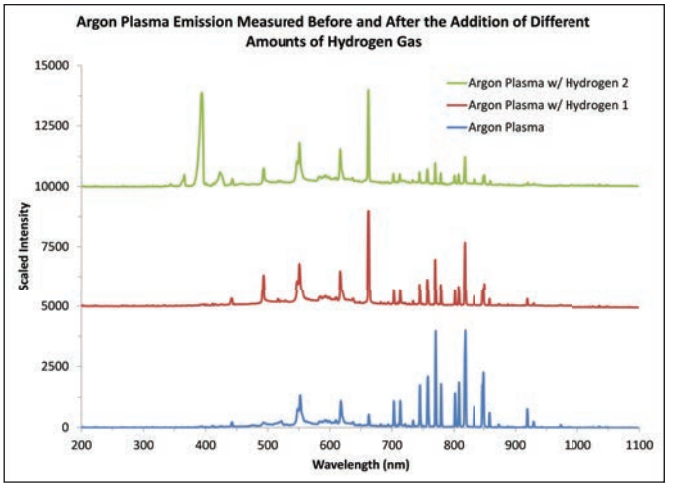

Figure 1

Argon plasma emission measured through the window of a plasma chamber before and after the addition of different amounts of hydrogen gas.

Conclusions

As we have shown, modular spectroscopy measurements with a high resolution spectrometer can be used to monitor changes in argon plasma as conditions are changed in the plasma chamber. The emission spectra provide critical information on the state of the plasma and the specific elements present. These spectral differences could be used to determine critical plasma parameters to enable precise control of the conditions in the plasma chamber. ■

Ocean Optics, Inc.
830 Douglas Avenue
Dunedin, FL 34698
Tel: (727)-733-2447
Email: info@oceanoptics.com
Website: www.oceanoptics.com

QUANTITATIVE ANALYSIS OF CEMENT BY EDXRF SPECTROMETRY

Shimadzu Scientific Instruments

Abstract

This note presents an analysis of pressure-formed cement standard powder samples using energy-dispersive X-ray fluorescence spectrometry.

Introduction

High-accuracy quality control analysis of cement is typically conducted using a wavelength dispersive X-ray fluorescence spectrometer.[1] However, energy-dispersive X-ray fluorescence (EDXRF) spectrometers have become capable in recent years of analysis accuracy comparable to that of low-output wavelength dispersive type instruments. Not only do EDXRF instruments offer such conveniences as the ability to analyze powders as they are, their application range has significantly increased to now include the analysis of such substances as cement. This application introduces an example of the analysis accuracy an EDXRF spectrometer can obtain, using pressure-formed cement standard powder samples.

Methods/Conditions

Sample: NIST Certificate of Analysis Standard Reference Materials® Portland Cement. SRM 1880b, 1881a, 1884b, 1886a, 1887b, 1888b, 1889a.

Sample Preparation: Pressure forming was conducted using a vinyl chloride ring (inner diameter 35 mmφ), with a total pressure of 250 kN for 60 seconds. Table 1 shows the standard values.

Results

Calibration Curves: The calibration curve and accuracy (1σ) for each element are shown in Fig. 1.

Lower Limits of Detection: The lower limits of detection calculated using the above calibration curves are shown in Table 2.

References

1. ISO 29581-2, JIS R 5204. ■

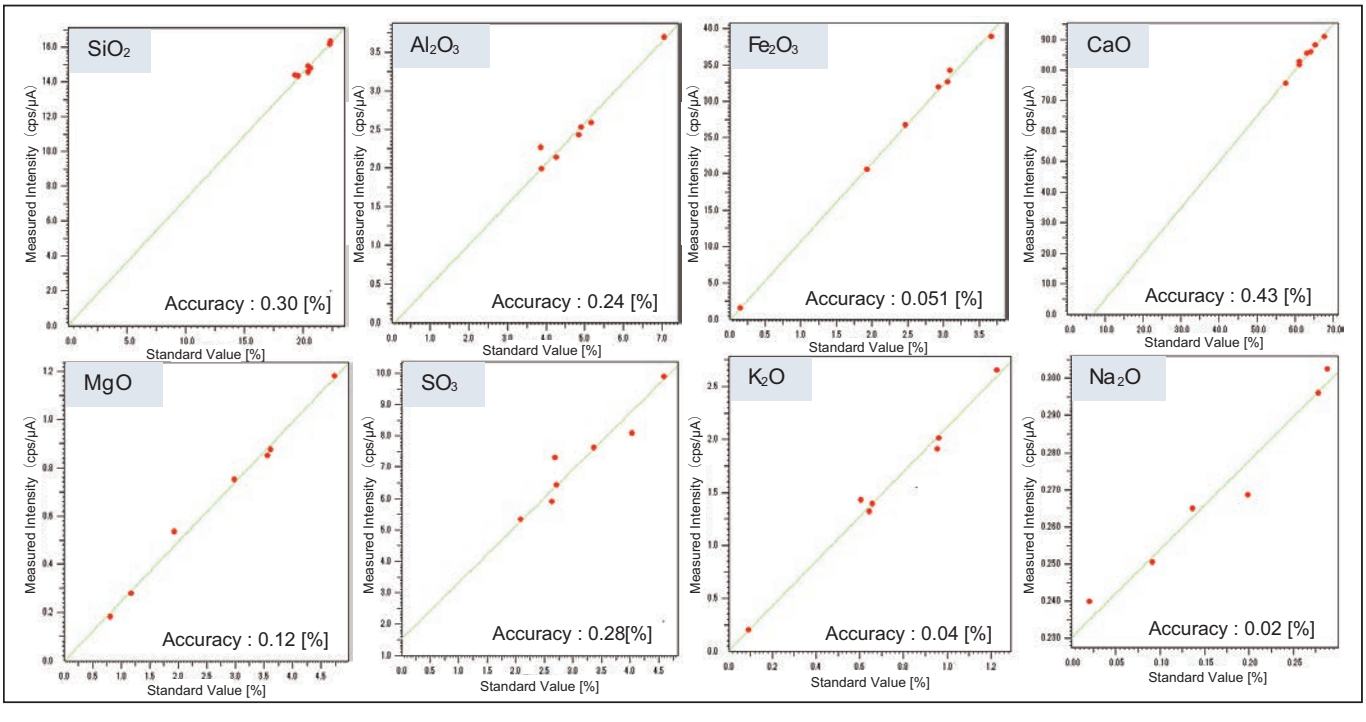

Figure 1
Calibration Curves and Accuracy.

22% of the Total Citations in Chemistry

Out of 152 journals in the category of multidisciplinary chemistry, ***JACS* is #1 with 431,286 total citations**, representing **22% of the citations** in the category. With a **10.677 Impact Factor**, ***JACS*** is the world's preeminent journal for all of chemistry and the interfacing areas of science.

ACS Publications
Most Trusted. Most Cited. Most Read.

Visit **pubs.acs.org/JACS** for more information.

Follow *JACS* on Twitter **@JACS**

Follow *JACS* at **facebook.com/JAmChemSoc**

Table 1: Standard Values

	SiO_2	Al_2O_3	Fe_2O_3	CaO	MgO	SO_3	K_2O	Na_2O
1880b	20.42	5.183	3.681	64.16	1.176	2.71	0.646	0.091
1881a	22.26	7.06	3.09	57.58	2.981	3.366	1.228	0.199
1884b	19.3	4.851	2.937	61.31	4.74	4.034	0.957	0.278
1886a	22.38	3.875	0.152	67.87	1.932	2.086	0.093	0.021
1887b	19.59	4.911	2.471	61.15	3.624	4.599	0.961	0.288
1888b	20.42	4.277	3.062	63.13	3.562	2.634	0.658	0.136
1889a	20.66	3.89	1.937	65.34	0.814	2.69	0.605	0.195

Table 2: Lower Limits of Detection (300 sec, 100 sec only for Fe_2O_3)

mass %	SiO_2	Al_2O_3	Fe_2O_3	CaO
Lower Limit of Detection (LLD)	—	0.0083	0.0022	—

mass %	MgO	SO_3	K_2O	Na_2O
Lower Limit of Detection (LLD)	0.0157	0.0066	0.0049	0.0159

SHIMADZU
Excellence in Science

Shimadzu Scientific Instruments
7102 Riverwood Drive
Columbia, MD 21046
Tel: (410) 381-1227
Website: www.ssi.shimadzu.com

SHIMADZU
Excellence in Science

The All-In-One Platform for FTIR Speed, Sensitivity, AND Resolution

Shimadzu's New IRTracer-100 Provides Exceptional Performance Across a Broad Range of Applications

With over 55 years' experience producing FTIR spectrophotometers, Shimadzu has cultivated a reputation for quality, delivering maximum performance and value. That quality continues. Introducing the **IRTracer-100**, a next-generation FTIR system from Shimadzu that redefines excellence in FTIR analysis.

Shimadzu's IRTracer-100 features:

- **High Speed:** Up to 20 spectra/second acquisitions
- **High Sensitivity:** Best-in-class 60,000:1 S/N ratio
- **High Resolution:** 0.25cm^{-1} resolution suitable for high-precision gas analysis
- **Easy Maintenance:** Automatic Dehumidifier and Advanced Dynamic Alignment features
- **Outstanding Reliability:** Self-diagnostics and validation routine

Learn more about Shimadzu's IRTracer-100.
Call (800) 477-1227 or visit us online at
www.ssi.shimadzu.com/Tracer

Optimized for network applications, new LabSolutions IR Software features an intuitive user interface as well as an extensive library of spectra and a high-performance search function. User-friendly macro functions automate routine work for enhanced work efficiency. In addition, numerous optional programs are available to address all modern laboratory needs.

Order consumables and accessories on-line at http://store.shimadzu.com
Shimadzu Scientific Instruments Inc., 7102 Riverwood Dr., Columbia, MD 21046, USA

SAXS ANALYSIS OF WEAKLY SCATTERING SURFACTANT MICELLES ON A LABORATORY X-RAY DIFFRACTION SYSTEM

Joerg Bolze, Ph.D. PANalytical B.V.

Abstract

Micelles formed by SDS surfactant molecules in dilute aqueous solution were investigated with SAXS using ScatterX^{78} attachment for a laboratory XRD system. In spite of the inherently very low scattering intensity of this sample it was possible to obtain data on the Empyrean multi-purpose diffractometer that compare well with synchrotron results and that allow for the characterization of the micellar structure.

Introduction

Micelles are formed by the self-assembly of amphiphilic molecules in a liquid medium. They have important technological applications e.g. in the detergent and pharmaceutical industries. As their application properties are closely related to their structure, control over and determination of the micellar structure is important. Small Angle X-ray Scattering (SAXS) is an ideal analytical technique for that purpose as it can be applied *in situ* and yields information not only about the size of the aggregates, but also about their internal structure and shape. However due to the weak scattering signal involved, this can only be done with advanced SAXS instrumentation.

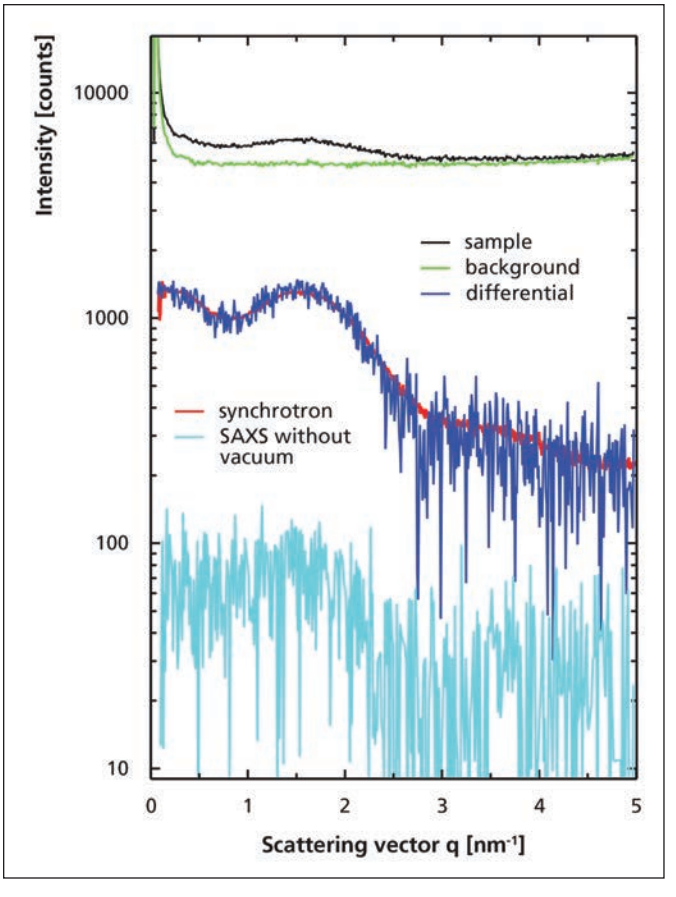

Figure 1

Sample and background measurements with ScatterX^{78} (30 min). The dark blue line is the differential scattering curve. Also shown are results from a measurement (8 h) without an evacuated beam path (light blue) and from a synchrotron SAXS experiment (red).

Methods/Conditions

SAXS data were acquired on the PANalytical Empyrean XRD platform configured with ScatterX^{78} evacuated SAXS attachment in combination with a focusing X-ray mirror and the PIXcel^{3D} solid state linear detector used in line mode. Sodium dodecyl sulfate (SDS) was dissolved in a 30 mM aqueous KCl solution to a concentration of 1.0 wt.%. The sample was loaded in a disposable quartz capillary and measured under ambient conditions. For the background measurement the capillary filled with the pure dispersion medium was used. Data reduction and analysis was done with the EasySAXS software.

Results: Part I

From Fig. 1 it is evident that the excess scattering intensity due to the presence of the micelles is extremely small. This is inherently due to their low concentration and small electron density contrast, making it challenging to separate the weak signal from the background. Meaningful data can only be obtained when counting statistics are good and with the background due to any parasitic scattering optimally suppressed. The background-corrected scattering curve obtained with ScatterX^{78} within only 30 minutes already shows distinct features that are in good agreement with synchrotron SAXS data [1]. The comparison also demonstrates the very good small-angle resolution that can be achieved. On the other hand, when measuring the same sample using a typical SAXS configuration without evacuated beam path and a point detector, too noisy data are obtained – even with a measurement time of several hours. For such weakly scattering samples it is essential to use an evacuated beam path and a low-noise line detector.

Model-Independent Data Analysis

By applying an indirect Fourier transformation on the experimental data, the corresponding pair distance distribution function *p(r)* could be determined. It contains the real space

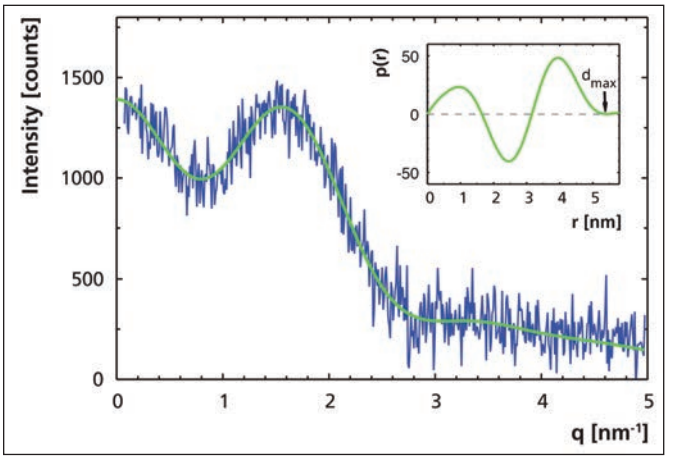

Figure 2
The inset displays the deduced pair distance distribution function p(r). In the main graph the scattering curve back-transformed from the p(r) function is compared with the experimental data, which were found to be in good agreement.

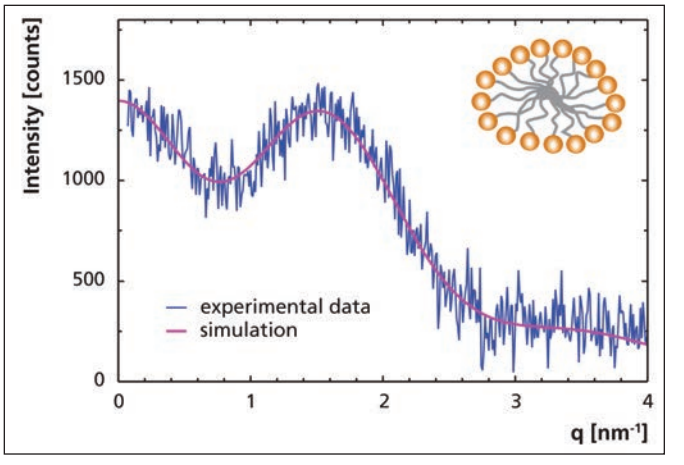

Figure 3
The experimental data compared with the result from a fit based on the model of core-shell ellipsoids. The inset shows the deduced aggregate structure of the micelles.

information of the scattering curve. Its characteristic shape points to a core-shell structure with a negative electron density contrast of the core, and a positive contrast of the shell. It is also in good agreement with what has been reported in the scientific literature [2]. The maximum dimension d_{max} of the micelle can be estimated from the point where *p(r)* levels off at zero (see Fig. 2).

Results: Part II

The experimental data could be fitted using the model of a prolate core-shell ellipsoid (see Fig. 3). The fit parameters are consistent with the known chemistry of the sample: the low-density core of the micelles is formed by the hydrocarbon chains of the surfactant molecules whereas the shell is occupied by the electron-rich, hydrophilic headgroups. They are also in good agreement with those reported in the scientific literature [2] based on experimental data that were acquired on a dedicated SAXS instrument.

Conclusion

The ScatterX^{78} attachment to the Empyrean multipurpose XRD platform is well suited for SAXS measurements on weakly scattering samples that normally required the use of dedicated SAXS instrumentation or even synchrotron radiation. The good sensitivity and small-angle resolution is achieved by using an evacuated beam path with focusing optics and advanced beam conditioning elements, combined with a zero-noise solid state line detector.

References

1. Courtesy of Prof. D. Svergun (EMBL, Hamburg). For the comparison the original synchrotron data were smeared with the instrumental resolution functions of ScatterX78 and scaled to the same intensities.
2. Narayanan, J. *et al.* A Small-Angle X-ray Scattering Study of the Structure of Lysozyme-Sodium Dodecyl Sulfate Complexes. *J. Coll. and Interf. Sci.* **328,** 67-72 (2008). And further ref. given therein. ■

PANalytical
117 Flanders Road
Westborough, MA 01581
Tel: (508) 647-1100
Website: www.panalytical.com

THERMOPLASTIC ELASTOMER FLOW PROPERTY DETERMINATION BY DYNAMIC RHEOLOGY

TA Instruments

Abstract

Rate-dependent viscosity data of thermoplastic elastomers is important for effective material property prediction and manufacturing process design. Rheological data also reveals compositional differences and the presence of a percolation threshold of the dispersed phase.

Introduction

Thermoplastic elastomers have gained considerable interest for their appealing combination of rubber-like final properties and convenient thermoplastic processing. Thermoplastic vulcanizates (TPV) are among the most prevalent thermoplastic elastomers for the replacement of cured rubber parts. Because TPV can be processed like thermoplastics, characterization of their flow behavior is critical to effective manufacturing design. Many TPV producers offer material grades based on both variable hardness and tailor-made processing types such as injection molding, blow molding or extrusion.

Methods/Conditions

Samples of TPV of varying composition were tested with the RPA elite oscillatory shear rheometer (TA Instruments, New Castle, DE USA). The RPA *elite* is a closed-cavity dynamic shear rheometer with grooved biconical dies designed for rubber and elastomer characterization. Pre-molded sample discs were used to improve homogeneity. Samples were loaded at 180°C and conditioned with a low strain and frequency (0.5%, 10 rad/s) for 10 minutes prior to data collection. Frequency sweep experiments were performed at 1% strain.

Results

The four tested samples of varying TPV composition each demonstrate the shear-thinning behavior which is common for polymers (Fig. 1a). At moderate to high frequencies (shear rates), the complex viscosity values are similar for each specimen. Larger differences become evident at low frequencies, which correlate with low shear rate behavior. The fourth sample (black curve) exhibits a Newtonian viscosity plateau at low frequencies.

Discussion

TPV are multiphase materials with a discontinuous cured rubber phase dispersed in a continuous polyolefin phase. The ratio of cured rubber to polyolefin is used to adjust the final hardness value; greater polyolefin content leads to higher hardness values. The specimen indicated by the black curve has a hardness value of 50 Shore D, indicative of a polyolefin-rich material. All other materials have hardness values from 50 to 75 Shore A and are rubber-rich materials. The viscous behavior of the low-hardness materials (high rubber-phase content) can be appropriately described by the Herschel-Bulkley model.

This model is specifically used for compounded materials such as rubbers and plastics with filler content above the percolation threshold. This model highlights a critical stress ($\sigma=\sigma_c+K(\dot{\gamma})^n$) at which the viscosity is infinite and under which the material does not flow, information that is particularly important for injection mold and extruder die design. The critical stress for rubber-rich TPV is clearly illustrated in Fig. 1b. This

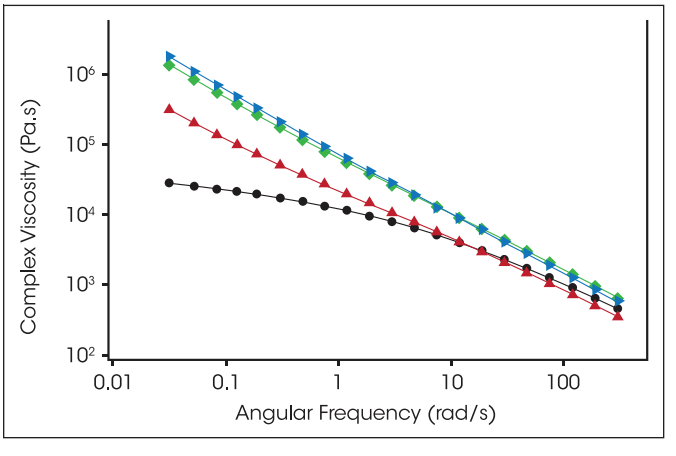

Figure 1a

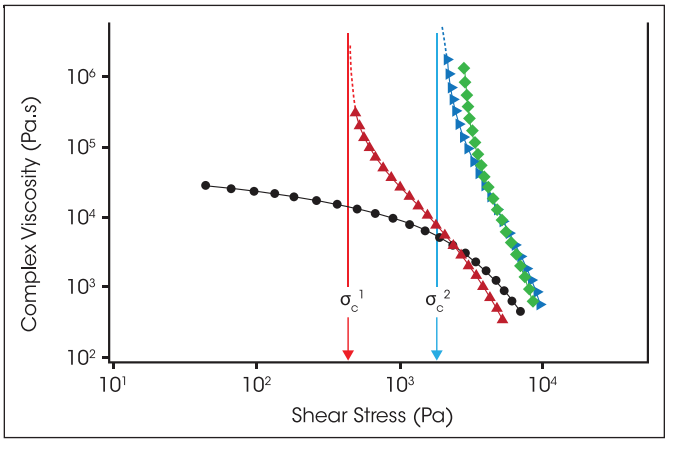

Figure 1b

representation of the data also reinforces the earlier conclusion that the polyolefin-rich material (black curve) does not exhibit a critical stress. ■

TA Instruments
159 Lukens Drive
New Castle, DE 19720
Tel: (302) 427-4000
Fax: (302) 427-4001
Email: info@tainstruments.com
Website: www.tainstruments.com

USING PRESSURE TO REDUCE BUBBLE CONTAMINATION FROM PARTICLE COUNT RESULTS

Dave Dunham Beckman Coulter Life Sciences

Introduction

Particle count data is a critical element to any fluid analysis program. This data can be used to identify maintenance intervals for heavy equipment, indicate the cleanliness level of fuel or the quality of hydraulic fluid used in an aircraft. Because of the potential impact on production uptime, costly physical assets and even human safety, having reliable data is crucial. Creating a sample prep SOP specific for your particle counting application (i.e. collection, agitation, degas, sample) is a critical first step. However, the presence of bubbles in sample fluid is something that nearly all particle counting applications have to contend with.

In an effort to enhance your sample prep SOP and the time required to get results, the HIAC 8011+ has incorporated a user configurable setting that pressurizes the sample chamber to a desired level and uses that pressure to "push" the sample through the Particle Counter Sensor. This unique process provides a couple advantages: It eliminates cavitation by using pressure as the sample delivery mechanism, plus, using pressure can reduce sample handling and provides results similar to the traditionally accepted method of using an ultrasonic bath. Once the desired pressure is reached in the sample chamber, sampling automatically begins, according to the sample recipe (SOP) created by the user.

Methods/Conditions

Analytical Conditions:

Recipe Name	Bubble Evaluation
Number of samples/run	3
Sample volume	5 ml
Tare	1.8 ml
Reporting Standard	Counts/ml
Channel sizes	2,3,4,5,7,12,14,21,25
System Pressure	80 PSI
Initial sample pressure	40 PSI

Prepare a Water Sample:

1. Blow out a new unused sample bottle for 5 seconds with clean dry air.
2. Fill the bottle to the shoulder with water and install into the 8011+.
3. Run the "Bubble Evaluation" Recipe.
4. Ensure this baseline run is saved to the USB drive.
5. Ensure the sample pressure is set to 50 PSI.
6. Prepare one of the bottles of sample fluid by performing the following:
   a. Handshake for one minute.
   b. Immediately install into the 8011+ sample chamber and run the "Bubble Evaluation" recipe.
   c. Ensure this bubble run is identified and saved to the USB drive.
   d. Re-shake the sample again for one minute.
   e. Degas for 25-35 seconds.
   f. Immediately install into the 8011+ sample chamber and run the "Bubble Evaluation" recipe again.
   g. Ensure this degassed run is saved to the USB drive
   h. Repeat procedure for 60, 70 and 80 PSI.

Results

Test data showed that as pressure in the sample chamber increased, particle counts decreased across all channel sizes. In samples where an ultrasonic bath was used during sample prep, additional improvement in count data was seen. Specifically, test data showed that use of an ultrasonic bath had a greater impact on count data on smaller channels (2,3,4μm). Comparing the data compiled in Tables 1 and 2, use of an ultrasonic bath had less of an impact on count data at channels $> 5\mu$m when compared to the data that used pressure alone. The count difference between these two methods on the larger channel sizes resulted in an average differential of 10% or <10 counts/ml across these channels.

As seen in Table 1, a significant count difference was realized when pressure was increased from 50 PSI to 80 PSI. Across all channels, counts decreased by an average of 31.7%

Table 1: Chamber Pressure and Ultrasonic Bath Count Data

Size	50 PSI	60 PSI	70 PSI	80 PSI	% improvement in counts
2	920	855	712	730	21%
3	522	479	399	389	25
4	331	307	253	241	27
5	147	132	109	96	35
7	136	123	100	87	36
12	87	77	60	54	38
14	5	4	3	3	40
21	1	2	0	0	100
25	0	1	0	0	NA

Table 2: Chamber Pressure Count Data

Size	50 PSI	60 PSI	70 PSI	80 PSI	% improvement in counts
2	828	865	828	812	2%
3	457	477	453	437	4
4	294	304	284	273	7
5	134	130	121	106	21
7	124	122	110	95	23
12	86	75	71	60	30
14	7	5	3	4	43
21	3	2	1	1	67
25	1	1	0	0	100

when an ultrasonic bath was used. Similarly, under worst case scenario conditions where a sample was shaken and introduced directly to the sampler, counts decreased by an average of 27.7% when pressure increased to 80 PSI.

Conclusions

The HIAC 8011+ has a configurable pressure setting that allows users to set the chamber pressure up to 90 PSI. Utilizing this feature allowed us to demonstrate that, for the samples under test, an increase in pressure resulted in a decrease in counts. The largest improvement in counts was seen in the larger sized channels; however, in the data set that required use of an ultrasonic bath, counts were reduced by up to 40%. Further, data indicates the even under worst case scenario conditions where a sample is agitated then placed directly into the sample chamber, significant improvements in count data are still seen. The ability to dial-in the optimum pressure for a particular fluid increases the precision of the data and reduces the potential for costly downtime. ■

Beckman Coulter Life Sciences
Particle Counting and Characterization
481 California Ave.
Grants Pass, OR 97526
Tel: (541) 472-6508
Email: CDDunhamIII@Beckman.com
Website: www.particle.com

MODULAR SPECTROSCOPY TOOLS FOR MEASURING INTRINSIC PROTEIN FLUORESCENCE

Yvette Mattley, Ph.D. Ocean Optics, Inc.

Abstract

In this application note, a UV LED and a high performance modular spectrometer were used to measure intrinsic fluorescence for the protein lysozyme in different conformational states. The objective was to demonstrate the power of modular spectroscopy for measuring inherent protein fluorescence to monitor changes in protein folding state.

Introduction

Proteins contain aromatic amino acids that fluoresce when excited with UV light. This intrinsic protein fluorescence depends on the amino acid composition and conformational state of the protein. As the protein goes from a native (folded) to a denatured (unfolded) state, the local environment surrounding the aromatic amino acids changes, affecting the fluorescence properties of the amino acids.

Proteins containing tryptophan and tyrosine (280 nm and 274 nm excitation, respectively), are best suited for UV excited fluorescence monitoring of protein conformation due to their relatively high quantum yield and similar excitation wavelengths. Phenylalanine is used less frequently for monitoring protein conformation because it has a much lower quantum yield with a lower excitation wavelength (~257 nm excitation).

The native state of a protein can be altered using elevated temperature, chaotropic or other chemical agents like urea or guanidine hydrochloride and changes in pH. As the protein unfolds, amino acids previously buried in the hydrophobic core of the protein are exposed to the solvent. Solvent exposure quenches the fluorescence of the amino acids and decreases the intensity of the intrinsic protein spectrum.

Methods/Conditions

A 280 nm UV LED was used with a high-sensitivity QE *Pro* spectrometer to measure fluorescence from samples of lysozyme diluted in neutral and acidic solutions. We prepared 3 mg/mL lysozyme (L6876 Sigma) in phosphate buffered saline (1X PBS pH 7.4) and 0.1 M HCl/KCl (pH 1) solution. Lysozyme suspended in 1X PBS was in its native (folded) state while lysozyme suspended in the acidic 0.1 M HCl/KCl solution began to denature and expose amino acids previously contained within the core of the protein to the solvent environment.

Results

The intrinsic protein fluorescence spectra for lysozyme diluted in 1X PBS (neutral pH) and 0.1 M HCl/KCl (acidic pH) are shown in Fig. 1. When lysozyme was exposed to low pH, the protein conformation changed exposing the tryptophan and tyrosine amino acids to a different environment. As a result, the fluorescence spectrum decreased in intensity as the protein changed from a folded conformation to an unfolded state.

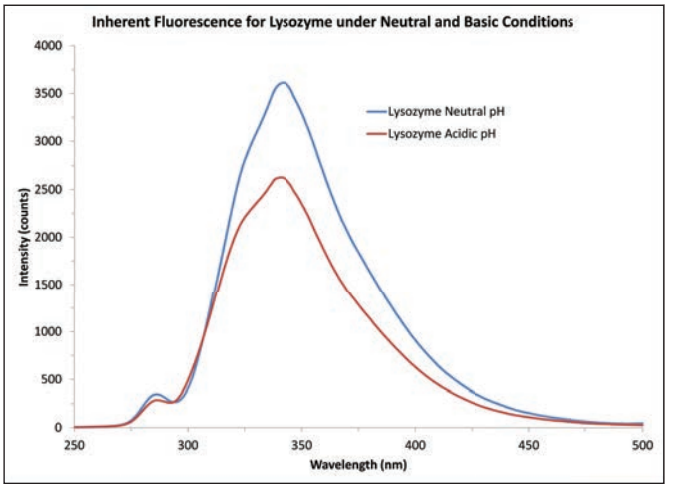

Figure 1
Changes in the fluorescence spectra of lysozyme with exposure to a low-pH.

Conclusions

Intrinsic fluorescence is a powerful indicator of protein structure and function. Inherent protein fluorescence can give researchers insight into the protein's conformational states and biological activity under different conditions including changes in temperature, pH and ion concentration. These changes in intrinsic protein fluorescence can be used to monitor protein unfolding for medical diagnostics applications where researchers are investigating neurodegenerative and other diseases associated with improper protein unfolding. ■

Ocean Optics, Inc.
830 Douglas Avenue
Dunedin, FL 34698
Tel: (727)-733-2447
Email: info@oceanoptics.com
Website: www.oceanoptics.com

RAMAN ANALYSIS OF ACTIVE PHARMACEUTICAL INGREDIENTS

Yvette Mattley, Ph.D. Ocean Optics, Inc.

Abstract

In this application note, we demonstrate the power of Raman spectroscopy through the measurement of two active pharmaceutical ingredients (APIs). The objective of the measurements was to show the rich information content of Raman spectra that gives it high specificity and the power to reliably identify compounds using their unique Raman spectral fingerprints.

Introduction

Raman spectroscopy offers a number of benefits for testing and characterization. It is rapid and non-destructive, requires limited to no sample preparation and allows for the measurement of solid or liquid samples. In addition, unlike near-infrared spectroscopy, Raman can be used to measure aqueous samples or samples with high moisture content. Measurements can also be made through sample packaging for samples contained in glass or even polymer packaging.

Raman is particularly useful for pharmaceutical applications. Raman techniques can be used to determine the characteristics of pharmaceutical raw materials, including active ingredients, binders, fillers, lubricants and other excipients. The ability to make Raman measurements through the walls of various pharmaceutical packaging makes Raman a great tool for noninvasive measurements of blister packs, pill bottles and vials.

Methods/Conditions

To illustrate the specificity and discriminating capabilities of Raman, we analyzed the active pharmaceutical ingredients acetaminophen and carbamazepine. Samples of the compounds in powder form were measured in standard, clear borosilicate scintillation vials. No additional sample preparation was needed.

Samples were analyzed using a modular Raman setup comprising a QE *Pro* Raman spectrometer, a 785 nm laser with 500 mW output and a fiber optic probe. The spectrometer covered the range from 150-2100 cm $^{-1}$ (780-940 nm) with approximately ~6 cm $^{-1}$ optical resolution. Samples were measured through the bottom of the vials at an integration time of 8 seconds with 3 scans to average.

Results

As demonstrated by the scaled spectra shown in Fig. 1, even though the active pharmaceutical ingredients have a similar appearance and chemical formula, Raman is able to go beyond the similarities for these compounds and probe their chemical structure to provide a unique spectral fingerprint for each compound. These fingerprints can then be used to identify the active pharmaceutical ingredients.

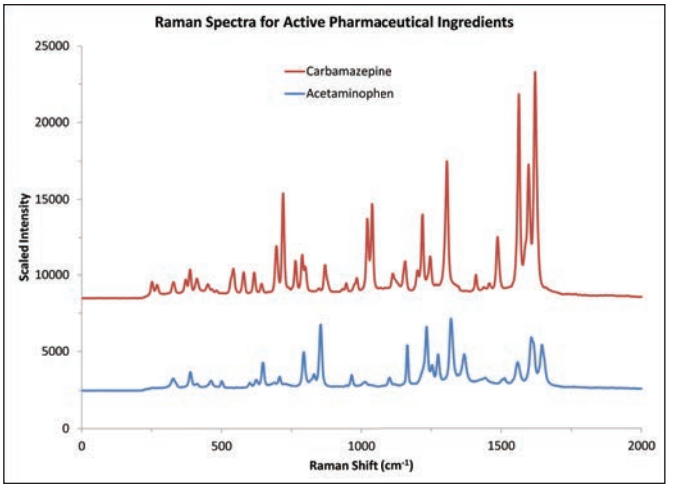

Figure 1
Raman spectra for active pharmaceutical ingredients acetaminophen and carbamazepine.

Conclusions

As we have demonstrated, Raman spectroscopy is a highly specific tool for the identification and discrimination of active pharmaceutical ingredients. The availability of both turnkey and modular Raman systems, complemented by sophisticated chemometric analysis packages and spectral libraries, makes Raman spectroscopy a versatile choice for a host of applications. With proper method development and application of chemometric analysis, Raman can even be used to obtain semi-quantitative data of active pharmaceutical ingredients in a pharmaceutical mixture. ■

Ocean Optics, Inc.
830 Douglas Avenue
Dunedin, FL 34698
Tel: (727)-733-2447
Email: info@oceanoptics.com
Website: www.oceanoptics.com

3D CONFOCAL RAMAN IMAGING OF AN EMULSION

WITec, GmbH

Introduction

Confocal Raman microscopy is a high-resolution imaging technique that has become widely used for the characterization of materials and specimens in terms of their chemical composition. With 3D Raman imaging, the chemical compounds and their distribution within the sample can be clearly illustrated.

Methods/Conditions

With a confocal Raman microscope a sample can be analyzed in steps along the optical axis to generate hyper-spectral 2D images, volume scans, and depth profiles. By taking a stack of images with different focal positions, the geometry of samples can be reconstructed in 3D. Fig. 1 shows such a 3D Raman image of a pharmaceutical emulsion. The data set was acquired, evaluated, and processed with the WITec Project FOUR software. At every image pixel a complete Raman spectrum was taken.

Results

The water and active pharmaceutical ingredient (API) containing phase is presented in blue, whereas with green the oil-matrix is displayed. In addition to the distribution of the known materials, silicone-based impurities could be visualized (red in the images). ■

For a 3D animation of Figure 1a go to: www.witec.de/assets/Videos/Figure1d_Emulsion_3D_Raman_image_WITec.gif

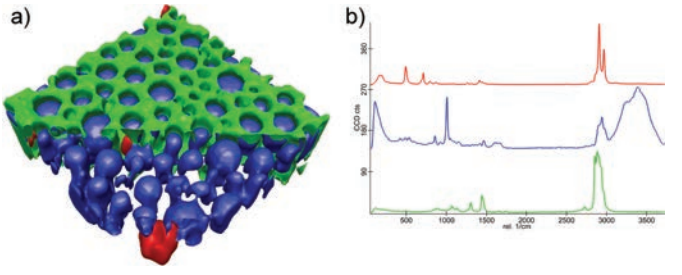

Figure 1

1a *3D Confocal Raman image of a pharmaceutical emulsion. Blue: Water and API, Green: Oil (information partially removed in the image), Red: Silicone impurities. Image parameters: 25 x 25 x 20 µm³; 200 x 200 x 50 pixels = 2,000,000 Raman spectra; integration time per spectrum: 10 ms; raw data file size: 6 GB.* ***1b*** *Corresponding Raman spectra with identical color-coding.*

WITec, GmbH
Lise-Meitner-Str. 6
89081 Ulm, Germany
Tel: +49 (0) 731 140 700
Fax: +49 (0) 731 140 70 200
Email: info@witec.de
Website: www.witec.de

INTEGRATION OF BENCHTOP NMR INTO UNDERGRADUATE CHEMISTRY MADE EASY

Mark Dixon Thermo Fisher Scientific

For professional educators of chemistry, crafting and maintaining laboratory classes is usually an evolutionary process where experience and success builds on itself to offer students the best experience possible. Part of that experience is providing hands-on access to analytical instrumentation, exploring problem-solving and logical cascades towards the correct interpretation. There is so much more to learn by *doing* rather than watching from a distance, or reading about how an analytical technique functions without context.

One such disruption is the recent and tantalizing prospect of owning an affordable benchtop NMR spectrometer, such as a Thermo Fisher Scientific picoSpin 45 or picoSpin 80, not previously available to the vast majority of educational institutions due to sky-high cost-of-entry and substantial cost-of-ownership of established NMR spectrometers designed around a cryogen-guzzling superconducting magnet.

Simply purchasing an NMR spectrometer and "plugging it in" to laboratory classes sounds simple enough … until one assesses the multitude of requirements that all need to fall neatly into place for NMR to be seamlessly integrated in a short amount of time. Often, the equipment is purchased just prior to the beginning of the next semester, and it is the responsibility of the teacher to get it up and running in a very short amount of time, a time which can be quite stressful if familiarity with NMR spectroscopy is not immediately forthcoming. Here are a few bullet points that help paint that picture:

- The NMR spectrometer should be proximal to the class, ideally in the same laboratory
- It should be portable enough to be removed and secured in between classes
- The instructor should be able to set up, maintain, and troubleshoot the spectrometer without the need for intensive training in either advanced electronics or administrative software
- Every student should be able to learn how to use the instrument quickly and easily, and only need training once
- The chemical information available from an NMR spectrum should be good enough for the problem in hand (i.e. resolution), and obtained quickly enough to lead the student to an answer within the laboratory class period (i.e. sensitivity)
- The lesson plans, and the molecules they start with and produce, should generate clear, unambiguous, and information-rich NMR spectra, easily interpretable by the student and the instructor

ISOPENTYL ACETATE

Abstract

Esters are a class of compounds found widely in nature. Low molecular weight esters tend to have characteristic flavors and pleasant odors that are most often associated with essential oils, even though essential oils are a complex mixture.

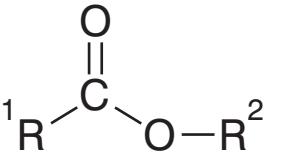

The purpose of this experiment is to synthesize isopentyl acetate (3-methylbutyl acetate) via an esterification reaction between acetic acid and isopentyl alcohol (3-methylbutanol), using concentrated sulfuric acid as a catalyst. The product will be washed, distilled, then characterized using NMR spectroscopy.

See the lesson plan here:
http://picospin.com/lesson-plans/synthesis-of-isopentyl-acetate-banana-oil/

Or view a detailed application note:
http://picospin.com/wp-content/uploads/2014/03/pS45-Fisher-Isoamyl-Acetate-Final.pdf

And it is this last bullet point that is most underestimated! If NMR was not used prior to buying the instrument, how is the educator to know if in-house lesson plans will comply to give complementary usable NMR information that FT-IR and UV machines may already provide? Furthermore, if they don't, where is the educator to go to find replacement lesson plans that work in the undergraduate environment (cost, safety, simplicity), from which NMR can be used as the tool for investigation?

At Thermo Fisher Scientific, we recognize the bind that an educator may find themselves in and have produced a set of complete lesson plans that contain all the information needed to answer that crucial question: what do I do if my existing les-

son plans need modifying to integrate NMR into my lab? They can be found at http://picospin.com/community. The collection will grow over time, with more and more customer contributions creating a valuable peer-to-peer forum.

As an example, the 'Fisher Synthesis of Banana Oil' lesson plan is typical of the collection available today and contains the following components:

- Introduction to the experiment and purpose of the lesson plan
- Full experimental details that can be used verbatim in the student's instructions
- How to prepare the NMR sample and acquire data on the picoSpin NMR spectrometer
- How to process and analyze the NMR data in Mnova (from Mestrelabs Research)
- A full interpretation of the results, translating spectral properties into chemical information
- Conclusions ■

Thermo
SCIENTIFIC
A Thermo Fisher Scientific Brand

Your NMR has arrived

In chemical education NMR spectroscopy is associated with providing definitive identification and comprehensive structural information. Unfortunately, it's also associated with large, costly and complex instruments. The Thermo Scientific™ picoSpin™ 45 NMR spectrometer creates a new paradigm with an award-winning design that is robust, affordable and accessible. With its bench-top size and weight, simplicity and reasonable price, the full-featured picoSpin 45 brings NMR spectroscopy to your lab and puts its analytical power into the hands of your students.

accessible, affordable, awesome

- See practical solutions for chemical education at thermoscientific.com/picospin

NEAR-INFRARED DIFFUSE REFLECTION FOR THE NONINVASIVE ANALYSIS OF FRUIT QUALITY

Yvette Mattley, Ph.D. Ocean Optics, Inc.

Abstract

In this application note, we evaluated the use of near-infrared (NIR) diffuse reflection measurements for the nondestructive measurement of avocados and mangoes. The objective of the measurements was to demonstrate the power of NIR spectroscopy for the noninvasive assessment of fruit quality.

Introduction

Consumers use many techniques to assess fruit quality including smell, firmness, sound, appearance and even intuition. These techniques work well in a grocery store setting but commercial fruit growers and packers require a more quantitative approach to determining fruit quality. Measurement of quality parameters such as sugar, starch and moisture content requires a rapid, noninvasive, online measurement to test fruit prior to picking or packaging. Analyzing these parameters through the peel of fruit or produce requires longer wavelengths that pass through the peel to measure the spectra for the fruit pulp beneath. NIR spectroscopy meets all these requirements.

Methods/Conditions

We measured NIR spectra for avocados and mangoes using the NIRQuest256-2.5 extended range NIR spectrometer (900-2500 nm) and Vivo direct illumination reflection stage. A 600 um fiber was arranged at 45 degrees relative to the halogen bulbs to measure diffuse reflection from the fruit relative to a diffuse reflection standard.

Results

The average of the spectra measured at four locations on each piece of fruit is shown in the figure for two mangoes and two avocados. Multiple spectra were recorded for each piece of fruit to account for the inhomogeneity of the fruit. While the spectral features are similar for both types of fruit, differences in intensity and spectral features are observed throughout the spectra. Sampling additional locations on the surface of the fruit would help to average out variability for a given piece of fruit and improve the accuracy and repeatability of the results.

Spectral features observed are a combination of light scattered from the surface of the fruit and light that passes through the peel where it is absorbed based on the chemical composition of the fruit. Fruit quality peaks of interest occur throughout the NIR spectral range with starch peaks near 1722 nm, 2100 nm and 2139 nm and sugar peaks between 900-1200 nm.

While the spectral data shown here illustrate the qualitative differences between avocados and mangoes, more quantitative information on fruit quality (sugar, starch and other fruit constituents) could be extracted from these spectra using an appropriate chemometric model and careful sampling to account for the inhomogeneity of the fruit.

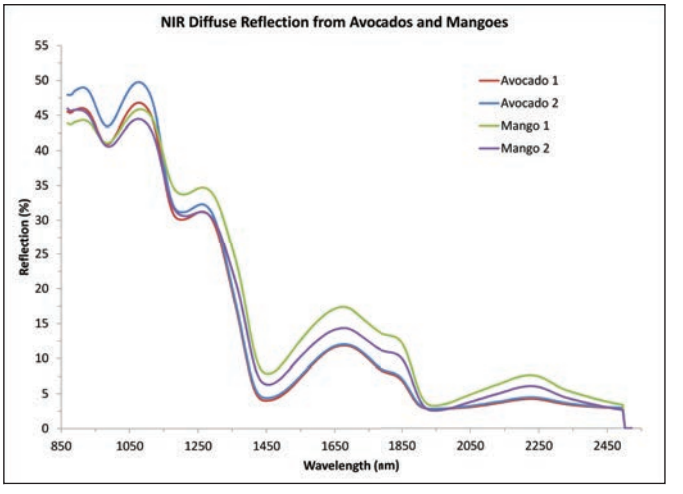

Figure 1

NIR diffuse reflection measurements of mangoes and avocados: Average of measurements from four different locations on each sample.

Conclusions

As we have demonstrated, NIR spectroscopy is a powerful measurement tool for the characterization of agricultural samples. In the case of fruit, long NIR wavelengths allow sampling through the peel of the fruit avoiding the need for sample preparation. With the ability to make rapid measurements of multiple parameters simultaneously, NIR spectroscopy is a great option for the nondestructive online measurement of fruit and produce. ■

Ocean Optics, Inc.
830 Douglas Avenue
Dunedin, FL 34698
Tel: (727)-733-2447
Email: info@oceanoptics.com
Website: www.oceanoptics.com

QUANTIFYING OLIVE OIL ADULTERATION WITH 60MHZ BENCHTOP NMR SPECTROMETRY

Nanalysis Corp.

Abstract

A calibration curve of manually adulterated olive oil was prepared by 1) determining the integration of the *bis*-allylic region relative to the total integration within each sample; and 2) plotting it versus the known amount of adulteration. The slope of this line can be used to determine the amount of soybean oil adulteration in an unknown.

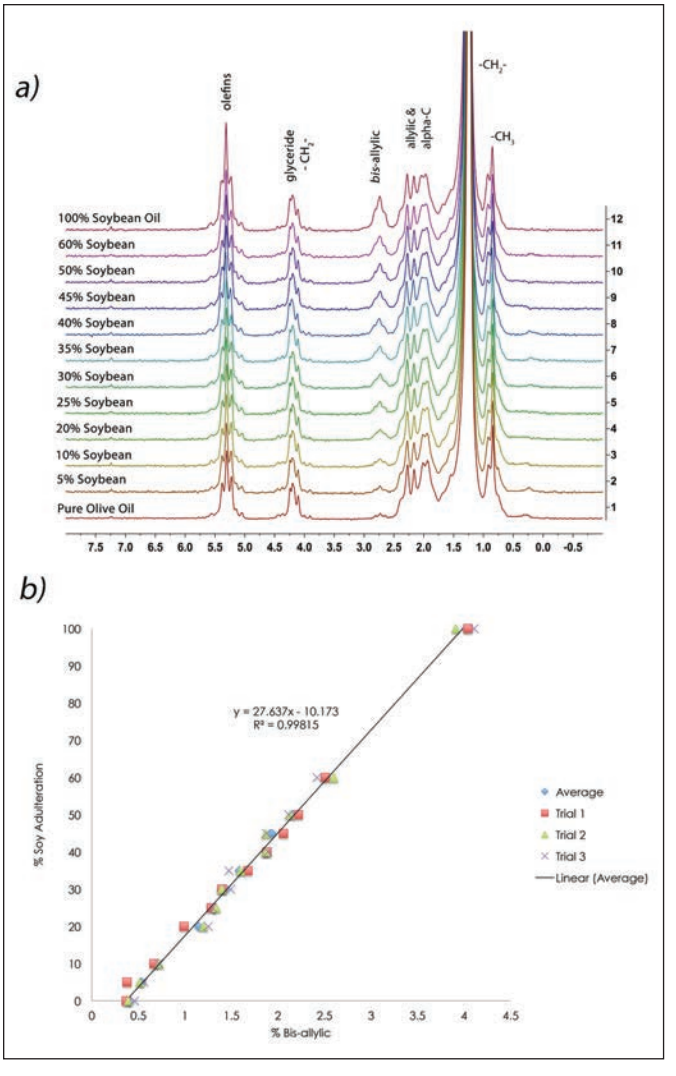

Figure 1

1a *Stacked ^{1}H NMR spectra of manually adulterated olive oil-soybean samples measured at 60 MHz.* ***1b*** *Amount of soybean oil adulteration as determined by the percentage of bis-allylic protons in each olive oil sample.*

Introduction

Olive oil has long been vulnerable to fraud. Methods to affirm and quantify adulteration typically utilize GC- or LC-MS. ^{1}H NMR spectroscopy offers an attractive alternative with linear response factors, fast sample preparation and simple data analysis. In this application note we highlight the efficacy of low-field, high-resolution benchtop NMR.

Methods/Conditions

0.5 M stock solutions of soybean and olive oil were prepared in *d*-chloroform and used to produce 0.5mL olive oil samples (0.5 mL in 5mm NMR tubes) at 0, 5, 10, 20, 25, 30, 35, 50, 45, 50, 60 and 100% soybean oil by volume. ^{1}H NMR spectra (8 scans, 5 second delay) were measured on the NMReady in triplicate for each sample.

Results

Fig. 1a shows a stacked plot of the ^{1}H NMR spectra for the oil samples integrated in regions: 'olefin' (δ 4.92 – 5.67), 'glyceride $-CH_2-$' (δ 3.82 – 4.5), *'bis*-allylic' (δ 2.50 – 3.05) 'allylic/alpha-C' (δ 1.75 – 2.50) and 'alkyl' (δ 0.46 – 1.75 ppm). As is consistent with the expected composition of fatty acids, and the higher composition of ω-3 and ω-6 fatty acids in soybean oil, there is a notable difference in the *bis*-allylic resonances between samples. For each spectrum, the percentage of *bis*-allylic protons was determined from the ratio of *bis*-allylic protons to the total sample integration. Plotting the percent of *bis*-allylic protons versus the amount of soybean adulteration affords a linear calibration curve (Fig. 1b). This curve can be easily used to quantify the amount of soybean oil adulteration in an unknown olive oil sample in less than a minute and within a few percent. ■

TWO EXCITATION WAVELENGTHS ARE BETTER THAN ONE

Frederick G. Haibach, Ph.D. and Huawen Wu, Ph.D. BaySpec, Inc.

Abstract

The ability to use two Raman excitation wavelengths in a single instrument improves both applicability and specificity on real-world samples. The gains are more than just a simple "sum of parts."

Introduction

Portable 785 nm and 1064 nm excitation wavelength dispersive Raman instruments have proven their worth in materials identification, especially for forensics, pharmaceutical raw materials inspection and first responders. Shorter wavelength excitation results in more efficient Raman scattering and allows the instrument designer to reduce the size and weight of the instrument. Longer wavelength excitation avoids exciting fluorescence that masks the Raman spectrum but the emphasis is on maximizing instrument throughput. Both approaches seek to maximize sensitivity and selectivity by different means.

Raman libraries are typically built using 1064 nm excitation FT-Raman instruments on purified materials and provide high-resolution, low-noise spectra. For portable applications, speed, weight and ruggedness and the ability to match FT-Raman libraries is ideal. Obtaining spectra quickly with a short-wavelength excitation Raman with baseline correction for fluorescence usually provides results about 70-80% of the attempts at measurement. Large amounts of fluorescence result in degraded match quality. Long wavelength excitation, while less efficient at creating Raman scattered photons, can produce fluorescence-free spectra for even colored materials. The identification rate for long-wavelength Raman is believed to be above 80%. Being able to use the best technique for each sample would be ideal.

An instrument designed around dual wavelength excitation can provide enhanced value beyond having two independent Raman instruments. The overall cost of the instrument can be significantly lower due to shared components between the two laser and spectrometer combinations. It also allows integration benefits like, a common user interface, shared Raman libraries and accessories, overlapping measurement volumes and even eliminating the need for recalibration when switching between spectrometers. With this level of integration, accuracy is maximized under all conditions.

Methods

Standard FT-Raman libraries [1] were adjusted to match the instrument response and line shape for both 785 and 1064 nm instruments. Spectra were taken of white and brown sugar. The colored compounds in brown sugar are the result of the Maillard and dehydration reactions and contain a complex mixture of compounds, including fluorescent furfurals. [2] Fluorescence is common in many colored materials. The match quality to the corresponding library spectrum is computed by the Pearson correlation coefficient, $R = (Lib \cdot Test)^2 / (Lib \cdot Lib)(Test \cdot Test)$.

Results

As shown in Fig. 1, the match quality for the 785 nm excitation spectrum is superior to the 1064 nm excitation spectrum for refined sugar because of the low noise and narrow line shapes. For brown sugar, a noisy spectrum is obtained using 785 nm excitation, but a definitive match to sucrose is seen with 1064 nm excitation despite the additional colored compounds.

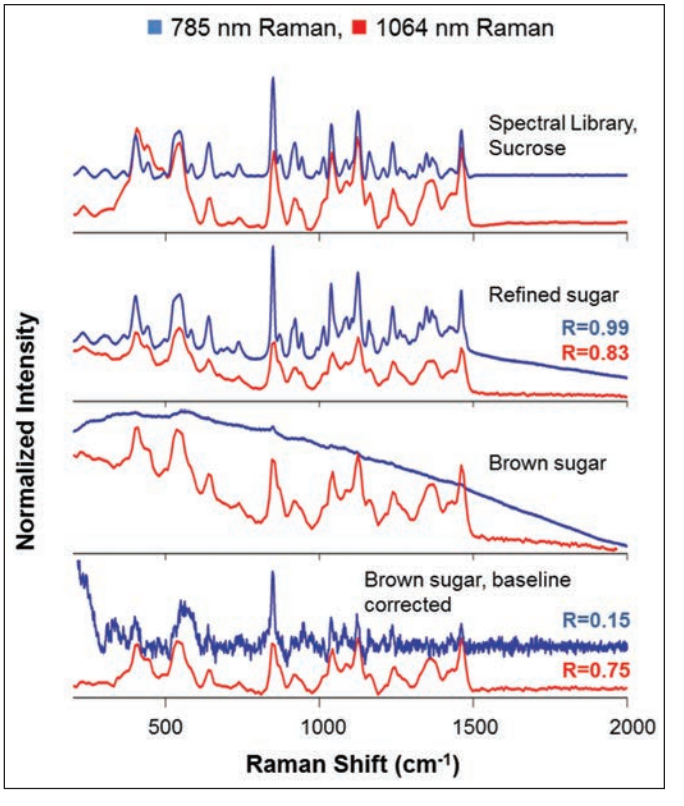

Figure 1

Discussion

Because of the resolution and improved Raman scattering efficiency, library matching using 785 nm excitation is preferred for low-fluorescence materials. However when fluorophores are present, significantly better Raman spectra can be obtained with longer-wavelength excitation.

A useful material identification library is composed of noise-free spectra of certified pure materials at a resolution appropriate to the destination instrument. Obtaining a low-noise spectrum from every sample is important to accurate identification. Using a highly integrated dual-band Raman instrument provides the opportunity to maximize results.

References

1. BaySpec Factory Library (2014).
2. Baunsgaard, D.; Nørgaard, L. and Godshall, M. A. *J. Agric. Food Chem.* **49,** 1687-1694 (2001). ■

RAMAN ANALYSIS OF BIODIESEL AND PETROLEUM-BASED FUELS

Yvette Mattley, Ph.D. Ocean Optics, Inc.

Abstract

In this application note, we measure spectral data for petroleum and biodiesel fuels. The objective of the measurements was to demonstrate the specificity and information content of the Raman spectra for these fuels.

Introduction

Biodiesel is a non-petroleum-based diesel fuel made from vegetable oil or animal fats. With growing interest in renewable energy sources, which are less toxic and have lower emissions than petroleum-based sources, production of biodiesel is on the rise. As this production increases, there are many opportunities to use Raman spectroscopy to assess the incoming raw materials, monitor the production process and confirm the quality of the final product.

Raman spectroscopy is an excellent technique for the identification and characterization of fuels. With no requirement for sample preparation and the power to identify and quantify materials using robust, handheld, portable instrumentation, Raman has found many uses in a range of industries. In the case of fuels, Raman spectra contain a wealth of spectral features due to the presence of different types of hydrocarbons resulting in a unique Raman fingerprint based on composition and chemical structure.

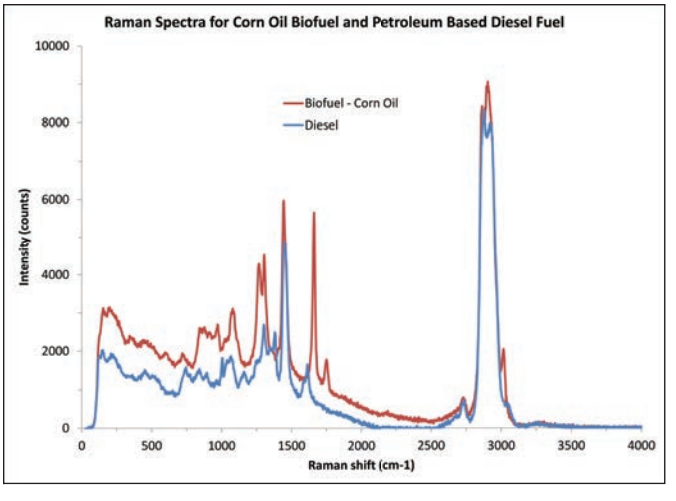

Figure 1
Raman spectra for corn oil biofuel and petroleum-based diesel fuel acquired with 785 nm laser excitation.

Methods/Conditions

We made Raman measurements for fuels using a Maya2000 Pro-NIR spectrometer, a 785 nm laser with 500 mW output and a fiber optic probe. A 500 millisecond integration time with no scans averaged and no boxcar smoothing were used. Samples of corn oil (diesel alternative) and petroleum-based diesel fuel were placed in small glass vials for analysis to illustrate the power of Raman to distinguish fuels and to characterize biodiesel raw materials.

Results

The Raman spectra for corn oil and diesel are shown Fig 1. While these spectra share some common features due to the hydrocarbon content of the samples, there are also a number of spectral differences observed in the fingerprint region from 500–2000 cm $^{-1}$. Even though both samples are suitable for use as fuel in diesel engines, they have distinct Raman spectra that distinguish the biodiesel fuel (corn oil) from the petroleum-based diesel fuel. Specifically, the presence of peaks for stearate (a form of the fatty acid found in animal and vegetable fats and oils) in the region from 1600-1800 cm $^{-1}$ are specific for corn oil and are not observed in the Raman spectrum for petroleum-based diesel fuel. These peaks along with the other spectral differences allow for easy discrimination of these fuels.

Conclusions

As we have shown, the unique hydrocarbon compositions of fuels make them well suited for identification and characterization using Raman analysis. The wealth of spectral features in the Raman spectra for fuels can be used in a range of applications including determination of critical fuel parameters, fuel classification and detection of counterfeit fuels. While the setup described here is one possible set of tools for Raman measurements, there are a number of other possibilities, both integrated and modular, to enable a range of measurements for different sample types and conditions. ■

Ocean Optics, Inc.
830 Douglas Avenue
Dunedin, FL 34698
Tel: (727)-733-2447
Email: info@oceanoptics.com
Website: www.oceanoptics.com

What makes spaceflight possible?

SCIENCE CAN BE TRICKY.

FINDING THE BEST SCIENTIFIC TALENT DOESN'T HAVE TO BE.

Renowned scientist Robert Hutchings Goddard is widely credited with creating and building the world's first liquid-fueled rocket. It should be no surprise that Goddard was a member of the American Chemical Society, the world's largest scientific association. With a membership of more than 161,000, the ACS comprises the greatest concentration of scientific ingenuity – bar none.

So when you're looking for the very best minds in the world, come to the one place they all reside.

C&EN jobs

A career catalyst for the world's top scientific minds.

WORLD-CLASS RECRUITMENT SOLUTIONS NOW OPEN

To reach a recruitment specialist, call 1-866-537-1068 • For more information, visit: **www.CENjobs.org**